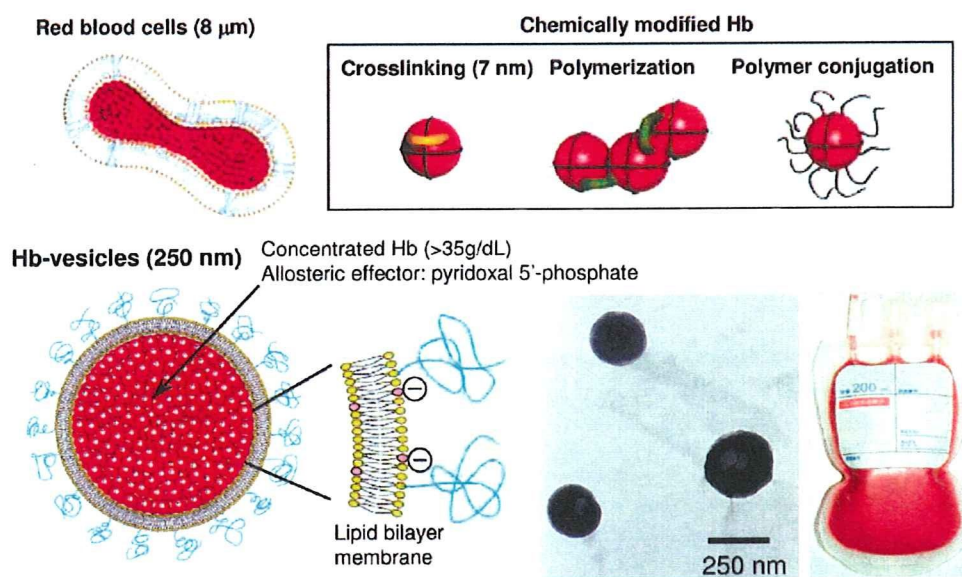
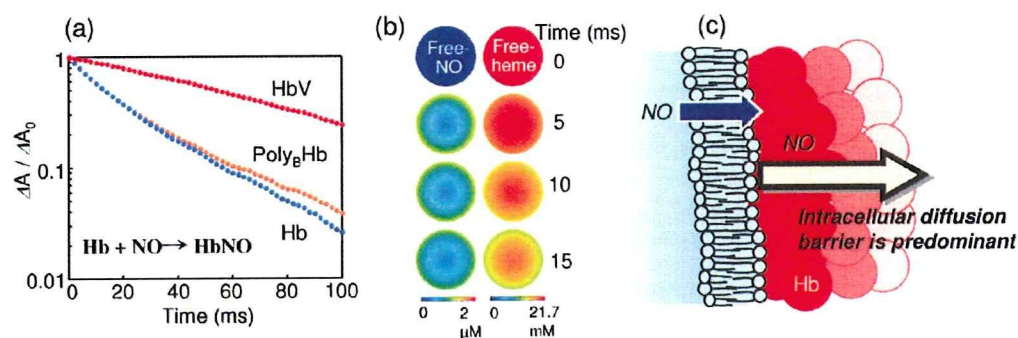


## Hemoglobin-based O<sub>2</sub> carriers



**Figure 2.** Schematic representation of a series of Hb-based O<sub>2</sub> carriers. Cross-linked Hb, polymerized Hb, and polymer-conjugated Hb are based on the chemical modification of Hb molecules (chemically modified Hbs). In the case of Hb-vesicles, a purified and concentrated Hb solution (35 g/dL) is encapsulated in phospholipid vesicles and the surface is modified using PEG chains. The particle size is well-regulated at 250 nm.



**Figure 3.** Encapsulation of Hb in vesicles retards NO binding. (a) Time courses of NO binding with HbV, human Hb with PLP (Hb/PLP = 1:2.5 by mol), and polymerized bovine Hb (Poly<sub>b</sub>Hb) observed by stopped-flow rapid scan spectrophotometry. The level of reaction was plotted on a semilogarithmic graph as a ratio of absorption at 430 nm ( $\Delta A$ ) at time  $t$ , to the initial absorption ( $\Delta A_0$ ) at time 0. NO-bubbled PBS ([NO] = 3.8  $\mu$ M) and deoxygenated-Hb-containing solutions in PBS ([heme] = 3.0  $\mu$ M) were mixed (31). (b) Schematic two-dimensional representation of the simulated time courses of distributions of unbound free NO and unbound free heme in one HbV (250 nm). Both free NO and unbound hemes are distributed heterogeneously. The concentration changes gradually from the surface to the core, indicating formation of the intracellular diffusion barrier (30). (c) The phospholipid bilayer membrane cannot have any barrier function to gas diffusion. The determinant factor of retardation of NO-binding should be the intracellular diffusion barrier, which was induced by (i) intrinsically larger binding rate constant of NO to a heme in an Hb molecule, (ii) numerous hemes as sites of gas entrapment at a higher Hb concentration, (iii) a slowed gas diffusion in the intracellular viscous Hb solution, and (iv) a longer gas diffusion distance in a larger capsule.

In 1957, Chang performed the pioneering work of Hb encapsulation to mimic the cellular structure of RBCs (35); microcapsules (5  $\mu$ m) were prepared using nylon, collodion, and other materials. Toyoda in 1965 (36) and the Kambara–Kimoto group in 1968 (37) also investigated encapsulation of Hbs with gelatin, gum arabic, silicone, and so forth. Nevertheless, results emphasized the extreme difficulty of regulating the particle size to be appropriate for blood flow in the capillaries and to obtain sufficient biocompatibility. After Bangham and Horne reported in 1964 (38) that phospholipids assemble to form vesicles in an aqueous medium and encapsulated water-soluble materials in their inner aqueous interior (39), it seemed reasonable to use such vesicles for Hb encapsulation. Djordjevich and Miller in 1977 (40) prepared liposome-encapsulated Hb (LEH) composed of phospholipids, cholesterol, fatty acids, and so forth. The US Naval Research Laboratories and collaborators demonstrated

remarkable progress in the use of LEH (41–43). Terumo Corp. (Tokyo) developed different LEH, so-called Neo Red Cells (44, 45) (Table 1).

However, some intrinsic issues of encapsulated Hbs remained, which were related mainly to the nature of molecular assembly and particle dispersion. What we call Hb-vesicles (HbV), with their high-efficiency production processes and improved properties, were established by our group based on technologies of molecular assembly in concert with precise analyses of their pharmacological and physiological aspects (46–48) (Tables 2 and 3). We use stable carbonylhemoglobin (HbCO) for purification with pasteurization at 60 °C for 10 h. The purity of the obtained Hb solution is extremely high (49, 50). Use of the stable and purified HbCO enables concentration of the Hb solution to more than 40 g/dL using ultrafiltration and easy handling of Hb encapsulation using the extrusion method,

**Table 1. List of Representative Liposome-Encapsulated Hbs (LEH) Extensively Studied Aiming at Industrialization and Other Potential Encapsulated Hbs Using Biodegradable Polymers**

product name	group	characteristics	current status
Hb vesicles (HbV)	Waseda Univ. and Keio Univ.	1. Pasteurization of HbCO at 60 °C for virus inactivation 2. Lipid composition to improve blood compatibility 3. PEG modification and deoxygenation for 2 yr storage 4. [Hb] = 10 g/dL	preclinical
Neo Red Cells (NRC)	Terumo Corp.	1. Inositol hexaphosphate to regulate $P_{50}$ (= 40–50 Torr) 2. Lipids: HSPC/cholesterol/fatty acid/PEG-lipid 3. Storage in a refrigerator for 6 months 4. [Hb] = 6 g/dL	preclinical
artificial red cells (ARC)	NOF Corp. and Waseda Univ.	1. Polymerized lipids (DODPC) for stabilization 2. Storage in powdered or frozen state 3. Difficulty in degradation in RES	suspended
liposome-encapsulated Hb (LEH)	US Naval Research Laboratory	1. Freeze-dried powder with trehalose 2. Low Hb encapsulation efficiency 3. Thrombocytopenia, complement activation	suspended
synthetic erythrocytes	Rush-Presbyterian-St. Luke's Medical Center, Univ. Illinois	1. The first attempt of LEH	suspended
Hb-loaded particles (HbP)	East China Univ. of Science and Technology	1. Hb encapsulation by poly( $\epsilon$ -caprolactone) (PCL) and poly( $\epsilon$ -caprolactone-ethylene glycol) (PCL-PEG) 2. Double emulsion and solvent diffusion/evaporation method 3. Biodegradable	basic study
polymersome-encapsulated Hb (PEH)	The Ohio State Univ.	1. Self-assembly of amphiphilic diblock copolymers composed of poly(ethylene oxide) (PEO), poly(caprolactone) (PCL), and poly(lactide) (PLA) 2. Biodegradable and biocompatible	basic study

**Table 2. Physicochemical Characteristics of Hb Vesicles**

parameter	
particle diameter	250–280 nm
$P_{50}$ (O <sub>2</sub> ) <sup>a</sup>	25–28 Torr
[Hb]	10 g/dL
[heme]	6.2 mM
[metHb]	<3%
[HbCO]	<2%
suspending medium	physiologic saline solution (0.9% NaCl)
colloid osmotic pressure	0 Torr
intracellular Hb concentration	ca. 35 g/dL
lipid composition	DPPC/cholesterol/DHSG/DSPE-PEG <sub>5000</sub>
$\zeta$ potential <sup>b</sup>	-18.7 mV
weight ratio of Hb to lipids	1.6–1.9 (w/w)
viscosity <sup>c</sup>	3.8 cP
lamellarity	nearly 1
stability for storage at room temperature	> 2 years, purged with N <sub>2</sub>
circulation half-life	35 h (rats)

<sup>a</sup> Measured with a Hemox Analyzer (pH 7.4, 37 °C). <sup>b</sup> Measured with a Zeta-Sizer Nano ZS ([NaCl] = 20 mM, pH 7.4). <sup>c</sup> Measured with Anton Parr Rheometer M301 (268 s<sup>-1</sup>, 25 °C).

**Table 3. Characteristics of Hb-Vesicles As a Transfusion Alternative**

- Human derived Hb solution is purified rigorously by pasteurization and ultrafiltration. The blood type antigens and pathogens are eliminated for utmost safety.
- Encapsulation of concentrated Hb solution (>35 g/dL), like RBCs.
- Small particle size (250 nm) for homogeneous distribution in the plasma phase of circulating blood.
- Shielding of the side effects of molecular Hbs by the lipid membrane.
- PEG modification for dispersion stability for long-term storage and in the bloodstream.
- Surface properties of HbV (PEG, negative charge, etc.) for blood compatibility.
- Prompt degradation and excretion of the components after entrapment in RES.
- Sufficient oxygen transporting capacity ([Hb] = 10 g/dL, cf, [Hb] of blood = 12–15 g/dL).
- Physicochemical properties are easily adjustable because of the nature of the "molecular assembly".

without causing Hb denaturation. It has been confirmed that HbV encapsulates nearly 35 g/dL within a thin bilayer membrane. In final processing, CO of HbCO in HbV is photodis-

sociated by irradiation of visible light under an O<sub>2</sub> atmosphere, and it converts to HbO<sub>2</sub> (57).

In fact, Hb autoxidizes to form metHb and loses its O<sub>2</sub>-binding ability during storage and during blood circulation (52–56). For that reason, metHb formation must be prevented. A method exists to preserve deoxygenated Hbs in a liquid state from using intrinsic characteristics of Hb: the Hb oxidation rate in a solution is dependent on the O<sub>2</sub> partial pressure; moreover, deoxyHb is not autoxidized at ambient temperatures (56). In the case of HbV, not only the encapsulated Hb but also the capsular structure (liposome) must be physically stabilized to prevent irreversible intervesicular aggregation, fusion, and leakage of the encapsulated Hb.

In addition to HbV, new encapsulated Hbs without liposomes have emerged with the use of recent advanced nanotechnologies, such as polymersome (57) and PEG-poly( $\epsilon$ -caprolactone) copolymer nanoparticles (58). In vivo evaluation of O<sub>2</sub>-carrying capacities of these new materials is anticipated. Encapsulation of Hb can reduce the toxicity of cell-free Hbs. However, numerous hurdles must be surmounted to realize encapsulated Hbs because of the components of the capsules themselves and their structural complexity as a molecular assembly. It is also important to consider the larger dosage requirement of encapsulated Hb for blood substitution than those of conventional drug delivery systems, which require no large dosage.

**2.2. Structural Stabilization and Destabilization using Polymerization or PEG Conjugation.** Liposomes, as molecular assemblies, have generally been characterized as structurally unstable. The US Naval Research Laboratory tested the addition of cryoprotectants and lyoprotectants such as trehalose to LEH for its preservation as a powder without causing hemolysis after rehydration (59, 60). In addition, many researchers have developed stabilization methods for liposomes that use polymer chains (61–64). Polymerization of phospholipids that contain two dienoyl groups (1,2-dioctadecadienoyl-*sn*-glycero-3-phosphatidylcholine; DODPC) was studied extensively by our group. For example, gamma-ray irradiation induces radiolysis of water molecules and generates OH radicals that initiate intermolecular polymerization of dienoyl groups in DODPC. This method produces remarkably stable liposomes, resembling rubber balls, which are resistant to freeze–thawing, freeze–drying, and rehydration (65, 66). Actually, the polymerized liposomes were so stable that they were not degraded easily in the macrophages,

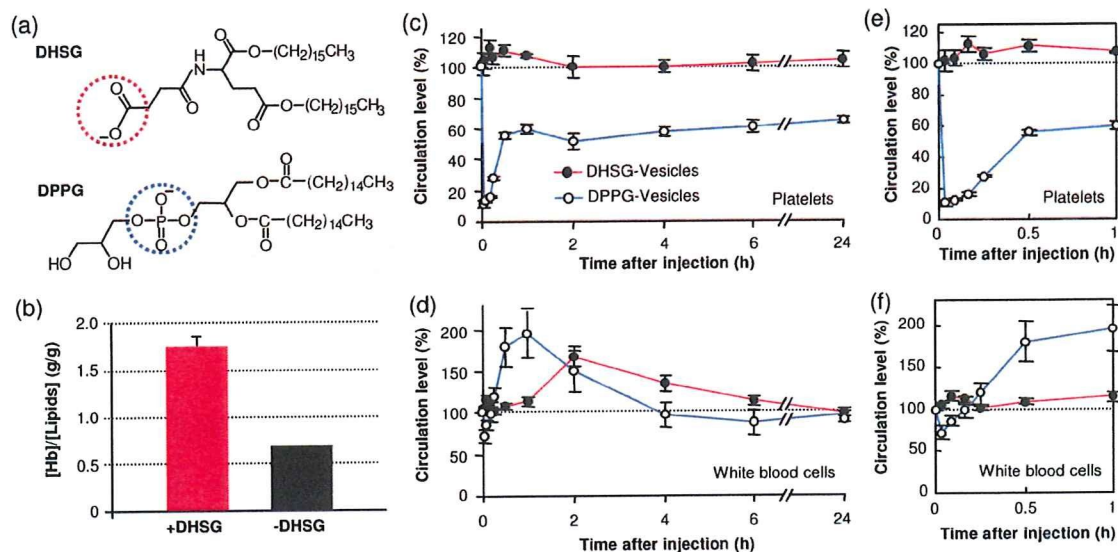


**Figure 4.** Effect of negatively charged vesicles on encapsulation capability and blood compatibility of HbV. (a) Chemical structures of negatively charged lipids, 1,5-*O*-dihexadecyl-*N*-succinyl-*L*-glutamate (DHSG) and 1,2-dipalmitoyl-*sn*-glycero-3-phosphatidylglycerol (DPPG). (b) Effect of DHSG on encapsulation efficiency of Hb (35 g/dL). (c–f) Circulation levels of platelets (c) and white blood cells (d) after intravenous infusion of vesicles containing 9 mol % DHSG (DHSG-vesicles) or 9 mol % DPPG (DPPG-vesicles) in rats (lipids; 280 mg/kg body weight). The right side graphs show the initial fluctuations in platelets (e) and white blood cells (f).

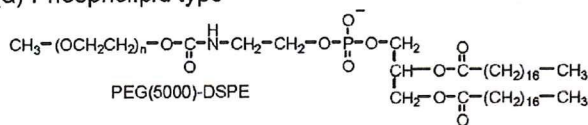
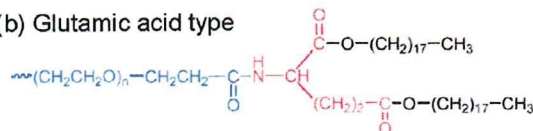
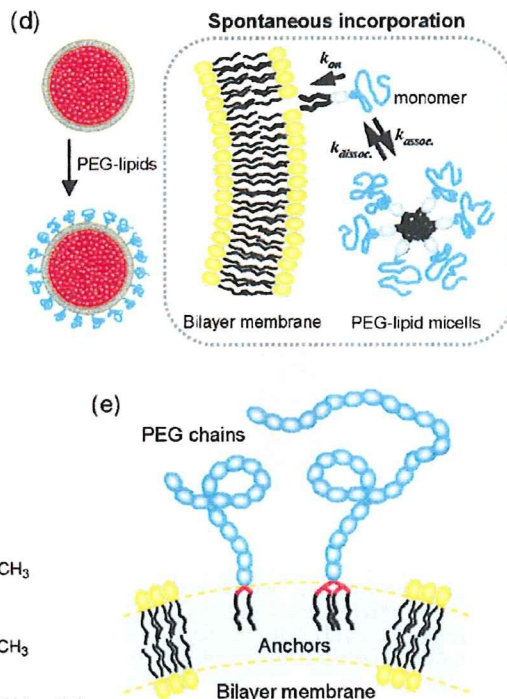
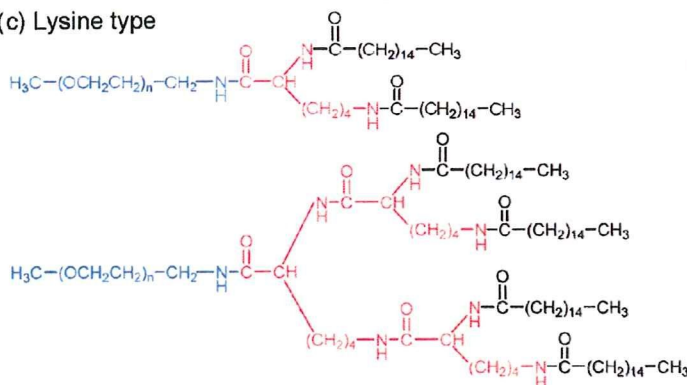
even 30 days after injection (67). It became widely believed that polymerized lipids are inappropriate for intravenous injection because of the difficulty in excretion. Subsequently, it was clarified that selection of appropriate lipids (phospholipid/cholesterol/negatively charged lipid/PEG-conjugated phospholipid) and that their composition is important to enhance the stability of nonpolymerized liposomes (45, 68). Surface modification of liposomes with PEG-conjugated lipids is sufficient for dispersion stability (69). In fact, in comparison to RBCs, HbV is highly resistant to hypotonic shock, freeze–thawing, and enzymatic attack by phospholipase A<sub>2</sub> (70).

We investigated the possibility of long-term preservation of HbV during storage for two years through a combination of deoxygenation and PEG modification (71). As little as 0.3 mol % PEG-conjugated lipid stabilizes the dispersion state and prevents aggregation and fusion for two years through steric hindrance (71–73). The original metHb content (ca. 3%) before preservation decreased gradually to less than 1% after 1 month because of the presence of a reductant, such as homocysteine, inside the vesicles that consumed the residual O<sub>2</sub> and gradually reduced the trace amount of metHb. The rate of metHb formation was strongly dependent on the O<sub>2</sub> partial pressure: a lack of increase in the metHb formation was observed because of the intrinsic stability of the deoxygenated Hb. In fact, the metHb content did not increase for two years. These results suggest the possibility that the HbV suspension can be stored at room temperature for at least two years, which would enable stockpiling of HbV for any emergency.

**2.3. Vesicular Surface Modification with PEG and Negative Charges for Blood Compatibility.** Liposome is not a solute: it is a particle in a suspension. The particle surface might be recognized, leading to interaction with blood components including complements. The so-called *injection reaction*, or pseudoallergy, results from complement activation, giving rise to anaphylatoxins, which trigger various hypersensitivity reactions. This reaction is observed sometimes not only with liposomal products (74), but also with fat emulsions (75), and a perfluorocarbon emulsion (76). Therefore, examination of blood compatibility of encapsulated Hbs is important for clinical use. Transient thrombocytopenia and pulmonary hypertension in relation to complement activation is an extremely important

hematologic effect observed in rodent models after infusion of LEH (containing DPPG: 1,2-dipalmitoyl-*sn*-glycero-3-phosphatidylglycerol) developed by the US Naval Research Laboratory (77, 78) and other products. In our group, exchange transfusion of prototype HbV (containing DPPG, no PEG modification) in anesthetized rats engendered transient thrombocytopenia and slight hypertension (79). Similar effects were also observed for administration of negatively charged liposomes (80, 81). The transient reduction in platelet counts caused by complement-bound liposomes was also associated with sequestration of platelets in the lung and liver. Such nonphysiological platelet activation probably engenders initiation and modulation of inflammatory responses because platelets contain several potent proinflammatory substances. A negatively charged lipid is required for encapsulating a large amount of Hb using a minimum amount of lipids (46–48). Therefore, we had to overcome the problem of conventional negatively charged vesicles to achieve blood compatibility. In the present formation of HbV, we use a negatively charged lipid (DHSG: 1,5-*O*-dihexadecyl-*N*-succinyl-*L*-glutamate) and confirmed the considerable improvement of Hb encapsulation efficiency (Figure 4a,b). It must be emphasized that the present vesicle formulation for HbV apparently does not induce thrombocytopenia or complement activation in animal experiments (Figure 4c–f) (82, 83), probably because the present HbV contains PEG-modification and a different type of negatively charged lipid (DHSG), not DPPG or a fatty acid.

Ikeda and his co-workers (83–86) thoroughly examined blood compatibility of HbV to human blood *in vitro*. The present PEG-modified HbV containing DHSG did not affect the extrinsic or intrinsic coagulation activities of human plasma, although HbV containing DPPG and no PEG modification tended to shorten the intrinsic coagulation time. The kallikrein-kinin cascade of the plasma was activated slightly by the prototype DPPG-HbV, but not by the present PEG-DHSG-HbV. The exposure of human platelets to high concentrations of the present HbV (up to 40%) *in vitro* did not cause platelet activation and did not adversely affect the formation and secretion of prothrombotic substances or proinflammatory substances that are triggered by platelet agonists. These results imply that HbV, at concentrations of up to 40%, has aberrant interactions with neither unstimulated

**Poly(ethylene glycol)-conjugated lipids****(a) Phospholipid type****(b) Glutamic acid type****(c) Lysine type**

**Figure 5.** Surface modification of HbV with PEG chains. (a–c) Chemical structures of PEG-conjugated lipids. (a) PEG(5000)-DSPE is commercially available and widely used for surface modification of lipid vesicles. (b) Glutamic acid-type and (c) lysine-type PEG-conjugated lipids were reported previously (87, 88). (d) PEG-modification of the HbV using the spontaneous incorporation of a PEG-lipid into the bilayer membrane (72). (e) Immobilization of the large water-soluble polymers on the bilayer membranes (87, 89).

nor agonist-induced platelets. It can be concluded that the present PEG-DHSG-HbV has higher blood compatibility.

For surface modification of HbV with PEG chains, several PEG-conjugated lipids having amino acid backbone have been synthesized, as presented in Figure 5b,c (87, 88). For other applications, these PEG-conjugated lipids are available to modify the surfaces of not only HbV but also lipid vesicles. Because the PEG-lipids having a large hydrophilic group form thermodynamically unstable self-assemblies, called micelles (73), they easily dissociate to monomers and spontaneously incorporate only to the outer surface of preformed HbV, as illustrated in Figure 5d (45, 72). Using this method, the required amount of PEG-conjugated lipid can be reduced by half or less because only the outer surface of HbV requires PEG chains. In addition, the PEG chains extending from the inner surface are expected to reduce the interior volume for encapsulation because of their exclusion volume effect. Therefore, modification only to the outer surface is important to encapsulate large amounts of Hb in lipid vesicles. To immobilize the hydrophilic macromolecules stably, such as PEG chains and proteins on lipid vesicles, a large hydrophobic anchor having a tetraacyl structure has been synthesized (Figure 5c,e). It has been confirmed that this hydrophobic anchor can stably immobilize PEG chains of high molecular weight ( $M_w$  12 500) or water-soluble proteins (87, 89). These surface modification technologies and lipid chemistry have been applied to the development of other functional biomaterials (87–93).

**2.4. Circulation Time, Biodistribution, and Metabolism.** The dosage of blood substitutes is expected to be considerably larger than those of other drugs, while their circulation time is considerably shorter than that of RBCs. Therefore, their biodistribution, metabolism, excretion, and side effects must be characterized in detail, especially in relation to the reticuloendothelial system (RES, alternatively, the mononuclear phagocytic system, MPS). Normally, free Hb released

from RBCs is bound rapidly to haptoglobin and is consequently removed from circulation by hepatocytes. However, when the Hb concentration is greater than the haptoglobin binding capacity, unbound Hb is filtered through the kidney, where it is actively absorbed. Hemoglobinuria and eventual renal failure occur when the kidney reabsorption capacity is exceeded. The encapsulation of Hb in vesicles completely suppresses renal excretion. However, HbV in the bloodstream is ultimately captured by phagocytes in the RES in much the same manner as senescent RBCs are, as confirmed by radioisotope  $^{99m}\text{Tc}$ -labeled HbV injection (42, 94). The circulation half-life is dose-dependent: for the dosage of 14 mL/kg body weight, the circulation half-life was 34.8 h in rats and 62.6 h in rabbits (Figure 6a). The HbV are finally distributed mainly in the liver, spleen, and bone marrow (Figure 6b). The species-dependent circulation time is inferred to be dependent upon the species-specific weight balance of phagocyte organs, particularly the liver, spleen, and bone marrow, against body weight (94). The circulation half-life in the case of the human body can be estimated as about 2–3 days at the same dosage.

It is generally accepted that the liposome clearance by RES at a small dosage is accelerated by opsonization (absorption of plasma proteins such as antibodies and complements on the liposomal surface). In fact, PEG-modification prevents opsonization for prolonged circulation times (95). However, considering a condition in which the dosage of HbV is extremely high and requires a considerable amount of opsonins, and in which HbV does not induce complementary activation (82, 83), then opsonin-dependent phagocytosis would not be a major component in the case of HbV with a large dosage. Actually, opsonin-independent phagocytosis, a direct recognition by macrophages, has been clarified in some studies (96, 97).

Analysis of the spleen by transmission electron microscopy (TEM) 1 day after infusion of HbV revealed the presence of HbV particles in the phagosomes of macrophages (98) (Figure

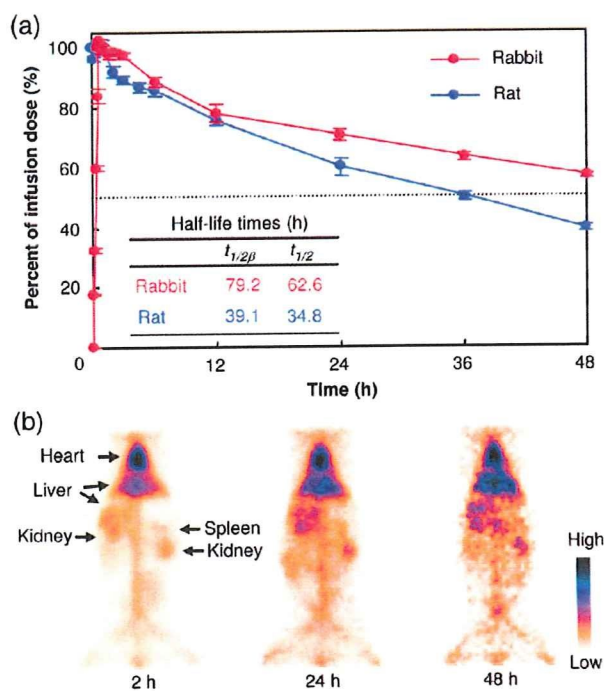


**Figure 6.** Circulation kinetics and organ distribution of HbV labeled with technetium-99m after top-loading intravenous infusion (14 mL/kg) in rats and rabbits (94). (a) Elimination profiles of HbV from blood. (b) Static gamma camera images of a rabbit acquired at 2, 24, and 48 h after HbV infusion.

7). However, after 7 days, the HbV structure cannot be observed. We confirmed transient splenomegaly with no irreversible damage to the organs and complete metabolism within a week. The phagocytic activity transiently, but not completely, decreased 1 day after injection, and it turned to increasing at 3 days. The influence on the defense function and its mechanism has been carefully examined in the ongoing research. Immunohistochemical staining with a polyclonal anti-human Hb antibody was used as the marker of Hb in the HbV. Results clarified that HbV had almost disappeared in both the spleen and liver after 7 days.

Bilirubin and iron are believed to be released during metabolism of Hb, but our animal experiments of topload infusion, daily repeated infusions, and 40% blood exchange showed that neither of those products increased in the plasma within 14 days (99–101). Bilirubin would normally be excreted in the bile as a normal pathway; no obstruction or stasis of the bile is expected to occur in the biliary tree. Berlin blue staining revealed considerable deposition of hemosiderin in the liver and spleen, even after 14 days. Moderate splenomegaly and hemosiderin deposition were also confirmed in the spleen after injection of stored RBCs, partly because of the accumulation and degradation of stored RBCs with lowered membrane deformability and shortened circulation half-life (101).

As for membrane components of Hb-vesicles, the plasma cholesterol level elevated transiently 3 days after injection: cholesterol was released from macrophages after degradation of HbV in phagosomes (99, 101). It was recently clarified using  $^3\text{H}$ -cholesterol that cholesterol of HbV is released from macrophages to blood; it is ultimately excreted in feces. The PEG chain is widely used for surface modification of liposomal products. The chemical cross-linker succinic acid ester of PEG-conjugated phospholipid is susceptible to hydrolysis to release PEG chains during metabolism. Actually, immunohistochemistry using an anti-methoxy-PEG antibody clarified that PEG had disappeared from the liver and spleen in one week (102). The

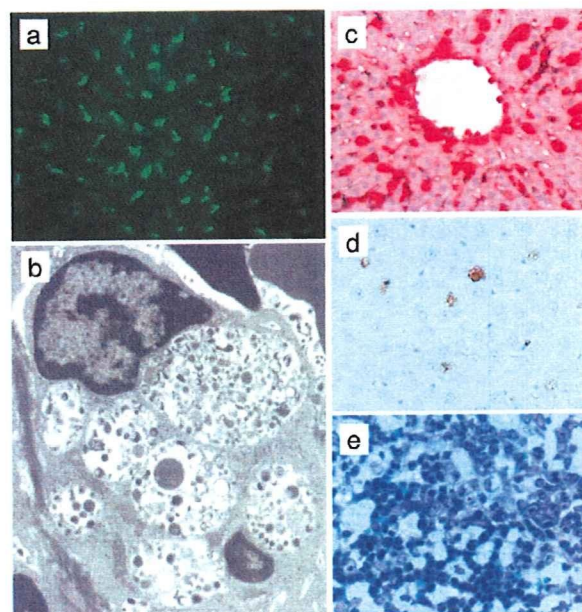


**Figure 7.** Histopathological examination of livers and spleens of rodents after injection of HbV. (a) Hamster liver 1 h after injection of fluorescence-labeled HbV, observed by a confocal laser scanning microscopy. The strong fluorescence indicates that HbV particles accumulate in Kupffer cells. (b) TEM of rat spleen macrophage 1 day after injection of HbV. The small black dots are HbV particles in phagosomes. The particles disappeared within a week (data not shown) (98). (c) Rat liver 1 day after injection of HbV. It was immunohistochemically stained with anti-human Hb antibody. The red parts indicate the presence of human Hb in HbV. It disappeared within a week (data not shown) (98). (d) Rat liver 7 day after injection of HbV. It was immunohistochemically stained with anti-methoxy-PEG antibody. The brown parts indicate the presence of PEG derived from PEG-lipid of HbV during the degradation. Fourteen days after injection, PEG was not detectable (data not shown) (102). (e) Rat spleen 3 days after 40% exchange transfusion with HbV. It was stained with Giemsa method. A large amount of blue cells, erythroblasts, are seen, indicating the enhanced hematopoiesis for the complete recovery of hematocrit within one week, while HbV are degraded in RES (101).

released PEG chains, which are known as inert macromolecules, are expected to be excreted in urine through the kidneys (103).

To determine the physiological capacity of RES for degradation of HbV, we tested massive intravenous doses by daily repeated infusion of 10 mL/kg body weight/day into Wistar rats for 14 days. The cumulative dosage was 140 mL/kg body weight (Hb and lipids, 20 689 mg/kg body weight). The total volume was equal to 2.5 times the total blood volume (56 mL/kg body weight) (100). Although splenohepatomegaly was considerable, all rats tolerated the infusions; their body weight increased during the succeeding 14 days until their intended sacrifice. The phagocytized HbV had disappeared, though the considerable hemosiderin deposition was confirmed in the spleen, liver, kidney, adrenal gland, and bone marrow. We were unable to define a lethal dose of HbV in this experiment.

The profile of liposome clearance is species-dependent. More precise data are necessary to extrapolate the phenomena observed in animal experiments to humans. However, these results imply that the metabolism of HbV and excretion are within the physiological capacity that has been well-characterized for the metabolism of senescent RBCs and conventional liposomal products.

**2.5. Regulation of  $\text{O}_2$  Transporting Capability (MetHb Reduction,  $\text{P}_{50}(\text{O}_2)$ ).** Actually, Hb encapsulation provides a unique opportunity to add new functions to particles by coencapsulation or embedding of functional molecules (52–56, 104–106). MetHb formation of HbV during the

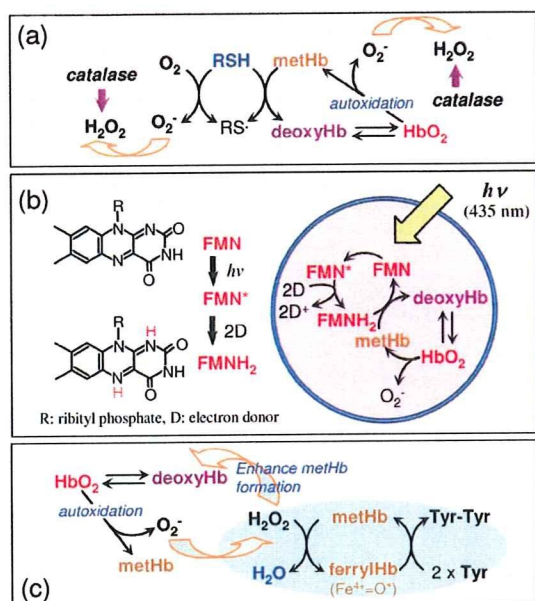


**Figure 8.** Artificial metHb reduction systems in HbV. (a) Coencapsulation of thiols (RSH), such as glutathione and homocysteine, reduces metHb. However, thiols react with  $O_2$  to generate  $O_2^-$  and  $H_2O_2$ . A more reactive thiol such as cysteine shows extremely rapid reaction with  $O_2$  and adversely facilitates metHb formation. Coencapsulation of catalase effectively eliminates  $H_2O_2$  and prevent such reactions (52, 53, 56). (b) Photoreduction system by coencapsulation of flavin mononucleotide (FMN) and an electron donor such as EDTA and methionine. Visible light irradiation (435 nm) primarily converts FMN to the photoexcited triplet  $FMN^*$ , and this reacts with two electron donors (D) to generate  $FMNH_2$ . MetHb is rapidly reduced once  $FMNH_2$  is produced (54). (c) During autoxidation of Hb and in blood circulation,  $H_2O_2$  is a potent metHb enhancer. A combination of L-tyrosine (Tyr) and metHb effectively eliminates  $H_2O_2$  and prolongs the functional lifetime of HbV (55).

preservation is completely prevented simply by deoxygenation. However, autoxidation of  $HbO_2$  is initiated once HbV is administered into the bloodstream because the entire metHb enzymatic system is eliminated during the Hb purification for the utmost safety from infection. An artificial metHb reducing system is required to prolong the  $O_2$ -carrying capacity of HbV. We have tested coencapsulation of reductants to directly reduce metHb and a photoreduction system using a photosensitizer such as flavin mononucleotide (FMN). A more practical method is to create an artificial enzymatic system using L-tyrosine (Tyr) and metHb that eliminates  $H_2O_2$  as does catalase (Figure 8).

Without a chemical modification of Hb,  $O_2$  binding affinity (expressed as  $P_{50}(O_2)$ ,  $O_2$  tension at which Hb is half-saturated with  $O_2$ ) of HbV can be regulated by coencapsulation of an allosteric effector (105, 106) (Figure 9a). The  $P_{50}(O_2)$  of purified Hb in a saline solution (in the presence of  $Cl^-$ ) is about 14 Torr; Hb strongly binds  $O_2$  and does not release  $O_2$  at 40 Torr (partial pressure of mixed venous blood). Historically, it has been regarded that the  $O_2$  affinity is expected to be regulated similarly to that of RBC, namely, about 25–30 Torr, using an allosteric effector or by a direct chemical modification of the Hb molecules. This enables sufficient  $O_2$  unloading during blood microcirculation, as evaluated by the arterio-venous difference in the levels of  $O_2$  saturation in accordance with an  $O_2$  equilibrium curve. Pyridoxal 5'-phosphate (PLP) is coencapsulated in HbV as an allosteric effector to regulate  $P_{50}(O_2)$  (105, 106). The main binding site of PLP is the N-terminal of the  $\alpha$ -chain and  $\beta$ -chain and  $\beta$ -82 Lysine within the  $\beta$ -cleft, which is part of the binding site of the natural allosteric effector, 2,3-diphosphoglyceric acid (2,3-DPG). The bound PLP retards the dissociation of the ionic linkage between the  $\beta$ -chains of Hb

during conversion of deoxy to oxyHb in the same manner as 2,3-DPG does. Therefore, the  $O_2$  affinity of Hb decreases in the presence of PLP. The  $P_{50}(O_2)$  of HbV can be regulated to 8–150 Torr by coencapsulating the appropriate amount of PLP or inositol hexaphosphate as an allosteric effector. Equimolar PLP to Hb (PLP/Hb = 1/1 by mol) was coencapsulated, and  $P_{50}(O_2)$  was regulated to 18 Torr. Furthermore,  $P_{50}(O_2)$  was regulated to 32 Torr when the molar ratio PLP/Hb was 3/1. The  $O_2$  affinities of HbV can be regulated easily without changing other physical parameters, whereas in the case of the other modified Hb solutions, their chemical structures determine their  $O_2$  binding affinities. Consequently, regulation is difficult. The present HbV contains PLP at PLP/Hb = 2.5 by mol; the resulting  $P_{50}(O_2)$  is about 25–28 Torr, which shows sufficient  $O_2$  transporting capacity as a transfusion alternative. Actually, HbV has been shown to provide  $O_2$ -transport capacity that is both sufficient and comparable to that of RBCs in experiments related to extreme blood exchange (68, 69, 79, 105, 107, 108) and fluid resuscitation from hemorrhagic shock (102, 109–112) (Figure 10). A recent experiment of HbV as a priming solution for cardiopulmonary bypass (CPB) in a rat model showed that HbV protects neurocognitive function by transporting  $O_2$  to brain tissue even when the hematocrit is reduced markedly (113).

The appropriate  $O_2$  binding affinities for  $O_2$  carriers have not yet been decided completely. However, the easy regulation of the  $O_2$  binding affinity might be useful to meet the requirement of clinical indications such as oxygenation of ischemic tissues. The  $P_{50}(O_2)$  of HbV without PLP and  $Cl^-$  is 8–9 Torr. This formulation is effective for targeted  $O_2$  delivery to anoxic tissues caused by reduced blood flow (107, 114, 115).

**2.6. Rheological Properties and Their Physiological Implications for Tissue Oxygenation.** The extremely high concentration of the HbV suspension ( $[Hb] = 10$  g/dL;  $[lipids] = 6$  g/dL, volume fraction, ca. 40 vol %) imparts an  $O_2$  carrying capacity that is comparable to that of blood. The HbV suspension does not possess a colloid osmotic pressure (COP), because one HbV particle (ca. 250 nm diameter) contains about 30 000 Hb molecules. In fact, HbV acts as a particle, not as a solute. Therefore, HbV must be suspended in or coinjected with an aqueous solution of a plasma substitutes. This requirement is identical to that for emulsified perfluorocarbon, which does not possess COP (116, 117); it contrasts to characteristics of other Hb-based  $O_2$  carriers, intramolecular cross-linked Hbs, polymerized Hbs, and polymer-conjugated Hbs, which all possess very high COP as protein solutions (15, 118) (Figure 9b).

Animal tests of HbV suspended in plasma-derived HSA or rHSA showed an  $O_2$  transporting capacity that is comparable to that of blood (110, 113). We reported previously that HbV suspended in plasma-derived HSA or rHSA was almost Newtonian: no aggregation was detected microscopically (68, 69). In Japan, rHSA was very recently approved for clinical use, in May 2008 (119), but various plasma substitutes are used worldwide, such as hydroxyethyl starch (HES), dextran (DEX), and modified fluid gelatin (MFG). The selection among these plasma substitutes is best determined not only according to their safety and efficacy, but also according to their associated price, experience of clinicians, and customs of respective countries. Water-soluble polymers generally interact with particles such as polystyrene beads, liposomes, and RBCs to induce aggregation or flocculation (120, 121). For that reason, it is important to determine the compatibility of HbV with these plasma substitutes. With that background, we studied rheological properties of HbV suspended in these plasma substitute solutions using a complex rheometer and a microchannel array (122). The rheological property of an Hb-based  $O_2$  carrier is important

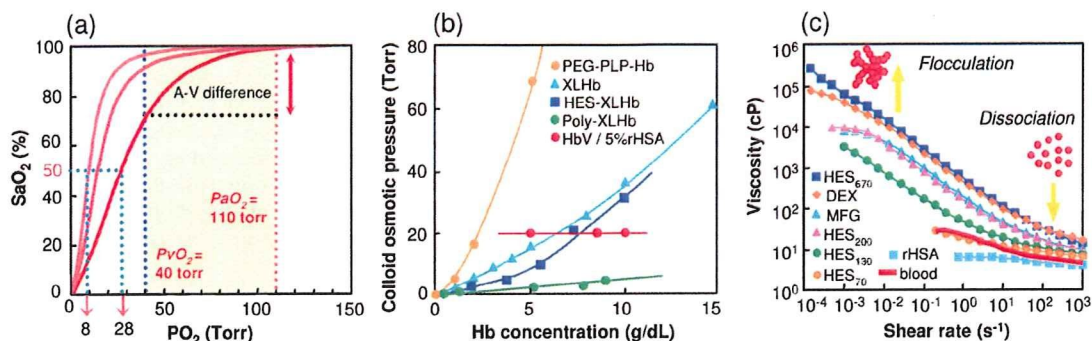


**Figure 9.** Regulation of physicochemical properties of HbV for versatile applications. (a) Oxygen dissociation curves of HbVs. Oxygen affinity ( $P_{50}$ , partial pressure of oxygen at which Hb is half-saturated with oxygen) is regulated by coencapsulation of PLP (105, 106). (b) Colloid osmotic pressure (COP) of chemically modified Hb solutions increase with the Hb concentration (15). In contrast, HbV particles have no oncotic effect. The figure shows 20 Torr when HbV is suspended in 5% rHSA. XLHb, intramolecularly cross-linked Hb. (c) Rheological properties of HbV suspended in various plasma substitute solutions (122). [Hb] = 10 g/dL, 25 °C.

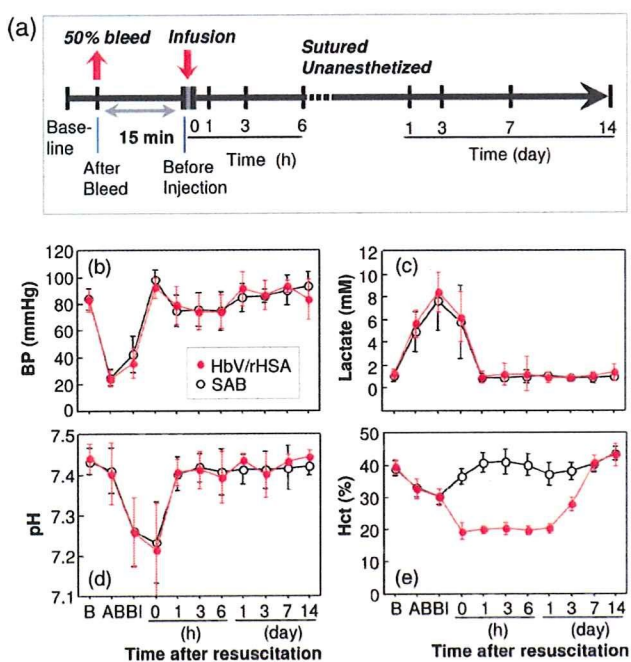


**Figure 10.** (a) Scheme depicting the experimental protocol of hemorrhagic shock and resuscitation (102). Shock was induced by withdrawing 50% of circulating blood volume from Wistar rats. After 15 min. they were resuscitated with either HbV suspended in recombinant human serum albumin (HbV/rHSA) or shed autologous blood (SAB). (b) blood pressure, (c) lactate, (d) pH, and (e) hematocrit (Hct). Mean  $\pm$  SD. B, Baseline; AB, after bleeding; BI, before injection (B-6 h,  $n = 24$ ; 1-14 days,  $n = 5$ ).

because the infusion amount is expected to be considerably large, which might affect the blood viscosity and hemodynamics.

The HbV suspended in rHSA was nearly Newtonian (Figure 9c). Its viscosity was similar to that of blood, and the mixtures with RBCs at various mixing ratios showed viscosities of 3–4 cP. Other polymers, HES, DEX, and MFG, induced flocculation of HbV, possibly by depletion interaction, and rendered the suspensions as non-Newtonian with the *shear-thinning* profile (122). These HbV suspensions showed high viscosity and a high storage modulus ( $G'$ ) because of the presence of flocculated HbV. On the other hand, HbV suspended in rHSA exhibited a very low  $G'$ . The viscosities of HbV suspended in DEX, MFG, and high-molecular-weight HES solutions responded quickly to rapid step changes of shear rates of 0.1–100  $s^{-1}$  and a return to 0.1  $s^{-1}$ , indicating that flocculation formation is both rapid

**Table 4.** Publications of Preclinical Studies Aiming at Applications of Hb-Vesicles for a Transfusion Alternative and for Oxygen Therapeutics

indication	ref
1. Resuscitative fluid for hemorrhagic shock	102, 109–112
2. Hemodilution	68, 69, 79, 101, 105, 107, 108
3. Priming fluid for extracorporeal membrane oxygenator (ECMO) for cardiopulmonary bypass	113
4. Perfusate for resected organs (transplantation)	24, 129
5. Oxygenation of ischemic brain (stroke)	130
6. Oxygenation of ischemic skin flap (plastic surgery)	115, 127, 128
7. Tumor oxygenation for sensitization to irradiation	131
8. CO carrier for cytoprotection at reperfusion	132

and reversible. Microscopically, the flow pattern of the flocculated HbV perfused through microchannels (4.5  $\mu m$  deep, 7  $\mu m$  wide, 20  $cmH_2O$  applied pressure) showed no plugging. Furthermore, the time required for passage was directly related to the viscosity.

It has been regarded that lower blood viscosity after hemodilution is effective for tissue perfusion. However, microcirculatory observation shows that, in some cases, lower “plasma viscosity” decreases shear stress on the vascular wall, causing vasoconstriction and reducing the functional capillary density (123). Therefore, an appropriate viscosity might exist, which maintains the normal tissue perfusion level. The large molecular dimension of HbV can result in a transfusion fluid with high viscosity. A large molecular dimension is also effective to reduce vascular permeability and to minimize the reaction with NO and CO as vasorelaxation factors (24, 25, 30, 31) (see Figure 3). These new concepts suggest reconsideration of the design of artificial  $O_2$  carriers (124). Actually, new products are appearing, although they are in the preclinical stage, not only HbV but also zero-link polymerized Hb (125) and others with larger molecular dimensions and higher  $O_2$  affinities (126). Erni et al. clarified that HbV with a high  $O_2$  binding affinity (low  $P_{50}(O_2)$ ), such as 8–15 Torr and high viscosity (such as 11 cP) suspended in a high-molecular-weight HES solution was effective for oxygenation of an ischemic skin flap (115, 127, 128). That study showed that HbV retains  $O_2$  in the upper arterioles, then perfuses through collateral arteries and delivers  $O_2$  to the targeted ischemic tissues, a concept of targeted  $O_2$  delivery by an Hb-based  $O_2$  carrier (114). A high  $O_2$  binding affinity (low  $P_{50}(O_2)$ ) would also be effective to improve the  $O_2$  saturation of Hb in pulmonary capillaries when exposed to a hypoxic atmo-

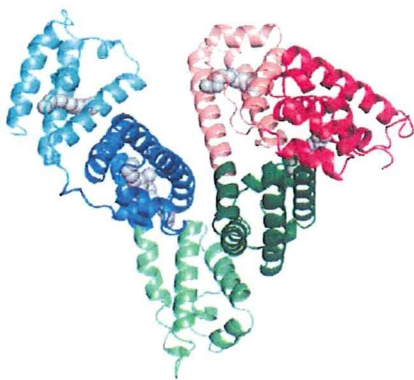


**Figure 11.** Crystal structure of HSA with myristate (PDB ID: 1BJ5) from ref (136).

sphere or with an impaired lung function. Some plasma substitutes cause flocculation of HbV and hyperviscosity. However, reports show that hyperviscosity would not necessarily be deteriorative and might be, in some cases, advantageous in the body (32). HbV provides a unique opportunity to manipulate the suspension rheology,  $P_{50}(\text{O}_2)$ , and other physicochemical properties, not only as a transfusion alternative, but also for other clinical applications such as oxygenation of ischemic tissues and ex vivo perfusion systems (129–132) (Table 4).

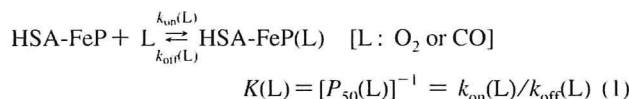
### 3. ALBUMIN-HEMES AS $\text{O}_2$ CARRYING PLASMA PROTEINS

**3.1. HSA Incorporating Synthetic  $\text{Fe}^{2+}$  Porphyrin (HSA-FeP).** HSA (Mw: 66 500) has a remarkable ability to bind a wide variety of exogenous compounds in the human circulatory system (133). This carrier protein comprises 3 homologue helical domains (I–III) with 9 loops formed by 17 disulfide linkages; each domain contains 2 subdomains (A and B) (Figure 11) (134–137). It is known that many common drugs such as warfarin, diazepam, and ibuprofen bind to one of the two primary sites (site 1 in subdomain IIA, site 2 in subdomain IIIA) (138). In fact, HSA helps to solubilize these compounds to achieve high concentration in the bloodstream; otherwise, they would easily aggregate and be poorly distributed.

In 1995, we found that tetrakis(*o*-pivalamido)phenylporphyrinatoiron bearing a covalently linked proximal imidazole (FeP1, Figure 12) was incorporated into HSA, yielding a red HSA-FeP1 hybrid (11). This synthetic hemoprotein can reversibly bind and release  $\text{O}_2$  under physiological conditions (pH 7.4, 37 °C) in much the same way as Hb. The HSA host adsorbs a maximal eight FeP1 molecules. Their stepwise binding constants ( $K_1$ – $K_8$ ) range from  $1.2 \times 10^6$  to  $1.2 \times 10^4$  ( $\text{M}^{-1}$ ) (Table 3) (139, 140). Solution properties of the HSA-FeP1 solution ( $[\text{rHSA}] = 5$  wt %,  $\text{FeP}/\text{HSA} = 1$ –8, mol/mol) are almost identical to those of HSA itself: the specific gravity, 1.013; viscosity, 1.1 cP; and COP, 20 Torr. Circular dichroism (CD) spectroscopy and isoelectric focusing measurement revealed that the second-order structure and surface charge distribution of HSA were unaltered after binding of FeP1. The obtained solution showed a long shelf-life of over two years at room temperature (141). Furthermore, HSA-FeP1 has no effect on the morphology of blood cell components (142) and does not engender immunological reaction and platelet activation (143). Upon addition of  $\text{O}_2$  gas through this solution, the visible absorption spectrum immediately changed to that of the  $\text{O}_2$  adduct complex. After exposure to CO gas, a stable carbonyl complex of HSA-FeP1 was formed (139, 140). The coordination structure of FeP1 and spin-state of the central ferrous ion was

characterized by IR, resonance Raman, and magnetic circular dichroism (MCD) spectroscopy (139, 140, 144). The carbonyl HSA-FeP1 moved to the NO adduct complex after bubbling NO gas (145). Subsequent ESR spectroscopy revealed that FeP1 in albumin formed a six-coordinate nitrosyl complex. The proximal imidazole moiety does not dissociate from the central ferrous ion when NO binds to the trans side (146).

The  $P_{50}(\text{O}_2)$  value of HSA-FeP1 is always constant (33 Torr, 37 °C) independent of the binding number of FeP1 (eq 1, Table 5)



The  $\text{O}_2$  binding equilibrium curve shows no cooperativity. However, the  $\text{O}_2$  transporting efficiency between the lungs [ $P(\text{O}_2)$ : ca. 110 Torr] and muscle tissue [ $P(\text{O}_2)$ : ca. 40 Torr] is 22%, which is identical to that for RBC.

The  $\text{O}_2$  association and dissociation rate constants [ $k_{\text{on}}(\text{O}_2)$  and  $k_{\text{off}}(\text{O}_2)$ ] can be measured using laser flash photolysis (147, 148). Interestingly, the rebinding process of  $\text{O}_2$  to HSA-FeP1 included two phases (fast and slow phase), perhaps because of the different environment around each FeP1 in the protein (149). The  $P_{50}(\text{O}_2)$  value can be controlled by tuning the chemical structure of FeP1. We have synthesized quantities of Fe(II)porphyrins (Figure 12) and evaluated the  $\text{O}_2$  binding parameters of their HSA-FeP hybrids (Table 6).

Actually, FeP2 has a bulky 1-methylcyclohexanamide group on the porphyrin ring plane (150). The  $\text{O}_2$  binding affinity of HSA-FeP2 [ $P_{50}(\text{O}_2)$ : 35 Torr] was almost identical to that of HSA-FeP1. However, the stability of the oxygenated complex increased to 4.5 times its usual value [half-life  $\tau_{1/2}(\text{O}_2)$ , 9 h; pH 7.3; 37 °C] (150).

In general, the basicity and structure of the proximal base greatly influences the  $\text{O}_2$  binding property of  $\text{Fe}^{2+}$ porphyrin. Both FeP3 and FeP4, similar analogues having an His ligand, showed high  $\text{O}_2$  binding affinities [ $P_{50}(\text{O}_2)$ : 3 Torr] (Figure 13, Table 6). Kinetically, substitution of the 2-methylimidazole to His reduces the  $\text{O}_2$  dissociation rate constant (150). Although one might think that high  $\text{O}_2$  binding affinity is not useful as a blood substitute, it can be efficient for oxygenation of hypoxic regions in tumors. Furthermore, the HSA-FeP4 showed long  $\tau_{1/2}(\text{O}_2)$  of 25 h (37 °C), which is 13-fold longer than that of HSA-FeP1.

Another HSA-FeP5, in which the active porphyrin has 3-methyl-L-histidine as a proximal base, exhibits an extraordinarily high  $\text{O}_2$  binding affinity [ $P_{50}(\text{O}_2)$ : 1 Torr] that approaches those of relaxed-state Hb and Mb (151). It is remarkable that replacement of the 3-methyl-L-histidine moiety by 1-methyl-L-histidine isomer (HSA-FeP6) reduced  $\text{O}_2$  binding affinity to 1/35th of its former level. The low  $\text{O}_2$  affinity of FeP6 is predominantly reflected by the high  $k_{\text{off}}(\text{O}_2)$  value. The axial Fe–N(1-methyl-L-histidine) coordination might be restrained by steric interaction between the 4-methylene group of the His ring and the porphyrin plane (151).

The proximal histidyl side chain can be introduced easily into the  $\beta$ -pyrrolic position of the porphyrin via an acyl bond in two steps, FeP7 (152). Although an electron-withdrawing acyl group is bound at the porphyrin periphery, the  $\text{O}_2$  binding affinity of HSA-FeP7 is slightly higher than that of HSA-FeP4. The rigid His-Gly(carboxy)butanoyl spacer of FeP7 probably produces a favorable geometry to fix the imidazole onto the central  $\text{Fe}^{2+}$  of the porphyrin.

Double-sided porphyrins (FeP8, FeP9, and FeP10) were also incorporated into HSA (153). We expected that steric encumbrances on both sides of the porphyrin enable the HSA-FePs to form a stable  $\text{O}_2$  adduct complex. Actually, the  $\tau_{1/2}(\text{O}_2)$  of HSA-



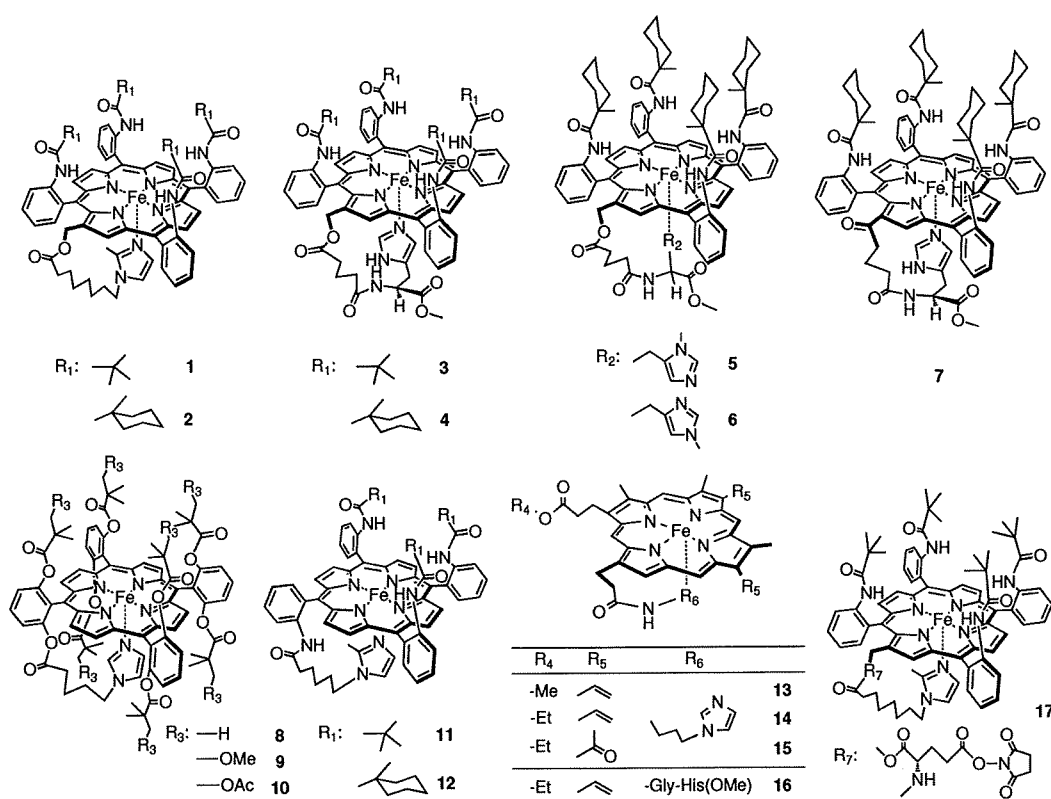


Figure 12. Structure of FePs in HSA-FePs.

Table 5. Solution Properties and Characteristics of HSA-FeP1

binding number of FeP1 ( $n$ )	1–8
binding constant of FeP1	$1.2 \times 10^6 - 1.2 \times 10^4 \text{ M}^{-1}$
$M_w$	$(66.5 + 1.3n) \text{ kDa}$
$pI$	4.8
viscosity <sup>a,b</sup>	1.1 cP
COP <sup>a,b,c</sup>	20 Torr
shelf life <sup>a,d</sup>	> 2 years

<sup>a</sup> In phosphate buffered solution (pH 7.3). [HSA]: 5 g/dL. <sup>b</sup> At 37 °C. <sup>c</sup> A membrane filter with a cutoff ( $M_w$ ,  $30 \times 10^3$ ) was used. <sup>d</sup> At 25 °C.

FeP8 was 5 h, which is 2.5-fold longer than that of HSA-FeP1. In addition, HSA-FeP8 showed high stability against hydrogen peroxide. The HSA incorporating double-sided porphyrins would be useful for the synthetic analogue of the oxidation enzyme.

Tailed porphyrins having an  $\alpha,\alpha,\alpha,\beta$ -conformer, FeP11 and FeP12, were synthesized easily via four steps from atropisomers of tetrakis(*o*-aminophenyl)porphyrin relative to eight steps of FeP1 (154). Although HSA-FeP12 binds  $O_2$  reversibly, HSA-FeP11 was quickly oxidized by  $O_2$ . We concluded that the 1-methylcyclohexanamide groups are necessary for the tailed porphyrin to form an  $O_2$  adduct complex under physiological conditions.

Investigations have also revealed that heme [ $Fe^{2+}$  protoporphyrin IX; protoheme] derivatives having a proximal base at the propionate side chain (FeP13–FeP16) were incorporated into HSA (155, 156). The oxidation process of HSA-FeP13( $O_2$ ) to the inactive ferric state obeyed first-order kinetics, suggesting that the  $\mu$ -oxo dimer formation was prevented by the immobilization of FeP13 into albumin. In fact, HSA-FeP15 showed lower  $O_2$  binding affinity [high  $P_{50}(O_2)$ ] than the others did. The acetyl groups at the 3,8-positions of FeP15 decrease the electron density of the porphyrin macrocycle, thereby reducing the  $O_2$  binding affinity. Actually, HSA-FeP16, in which the His-Gly tail coordinates to the  $Fe^{2+}$  center, showed the most stable

$O_2$  adduct complexes [ $\tau_{1/2}(O_2)$ , 90 min; pH 7.3; 25 °C] of any of these heme complexes.

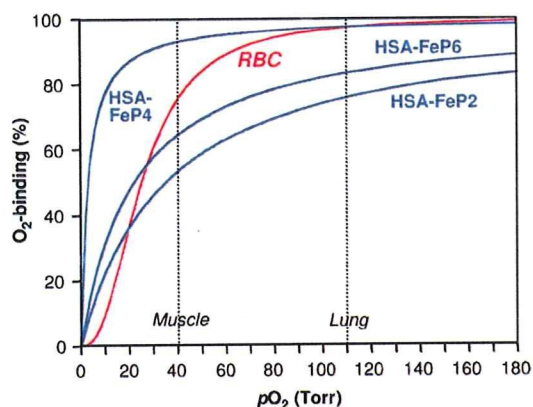
**3.2. Surface-Modified HSA-FeP with PEG.** A remaining defect of HSA-FeP is that the active  $Fe^{2+}$  porphyrin sites dissociate slowly from HSA when infused into animals because FeP is bound noncovalently to albumin. One possible solution is to bind the FeP molecule covalently to the protein. We have synthesized FeP17 having a succinimide side chain; it can react with the Lys amino group of HSA (157). The  $O_2$  binding property of HSA-FeP17 is almost identical to that of HSA-FeP1.

Another approach is surface modification with PEG. Actually, PEG decollations of proteins and liposomes are well-known to enhance their plasma half-life, thermostability, nonimmunogenicity, and solubility in organic solvents (158–163). We surmised that surface modification of HSA-FeP2 by PEG might help to prolong the circulation lifetime of FeP2 and retain its  $O_2$  transporting ability in vivo for a long period. Consequently, HSA-FeP2 (FeP2/HSA = 4/1, mol/mol) was modified with maleimide-PEG, and the solution properties,  $O_2$  binding behavior, and circulatory persistence of the PEG-modified HSA-FeP2 [PEG(HSA-FeP2)] were examined (164). A thiolation reagent, iminothiolane, first reacted with the Lys amino groups of HSA to create active thiols that bind to  $\alpha$ -maleimide- $\omega$ -methoxy PEG (Figure 14a). Mass spectroscopy measurements and quantification of the mercapto group of PEG(HSA-FeP2) revealed the conjugation of six PEG chains on the HSA-FeP2 surface. The initial FeP2/HSA ratio 4/1 (mol/mol) was unchanged after the PEG binding. The adjustment of viscosity is important to design an artificial  $O_2$  carrier. Maintenance of viscosity is necessary to preserve shear stress on the vascular wall that prevents loss of the functional capillary density (123, 165). The viscosity and COP of PEG(HSA-FeP2) were modulated to some degree by changing the molecular weight of PEG [ $M_w$ :  $2 \times 10^3$  (PEG<sub>M2</sub>) and  $5 \times 10^3$  (PEG<sub>M5</sub>)] (Figure 14b). In fact, PEG<sub>M2</sub>(HSA-FeP2) showed almost identical values of viscosity

**Table 6.** O<sub>2</sub> Binding Properties of HSA-FePs in Phosphate Buffered Solution (pH 7.3, 25 °C)

FeP	$k_{on}(O_2)$ ( $\mu M^{-1} s^{-1}$ )		$k_{off}(O_2)$ ( $ms^{-1}$ )		$P_{50}(O_2)^a$ (Torr)	refs
	fast	slow	fast	slow		
1	34	9.5	0.75	0.20	13 (33)	139, 149, 150
2	46	7.3	0.98	0.16	13 (35)	150
3	36	6.1	0.059	0.010	1 (3)	150
4	54	8.8	0.089	0.014	1 (3)	150
5	54	6.8	0.02	0.0024	0.2 (1)	151
6	54	8.1	0.62	0.093	7 (22)	151
7	34	4.5	0.045	0.0059	0.8 (2)	152
8	11	1.5	0.50	0.069	28	153
9	11	2.0	0.41	0.076	23	153
10	8.9	2.3	0.34	0.088	23	153
12	29	4.4	1.10	0.16	22 (45)	154
13	—	—	—	—	0.1	155, 156
14	—	—	—	—	0.1	155, 156
15	—	—	—	—	0.4	156
16	—	—	—	—	0.1	155, 156
17	28	—	0.33	—	9 (27)	157

<sup>a</sup> At 37 °C in parentheses.

**Figure 13.** O<sub>2</sub> binding equilibrium curve of HSA-FePs under physiological conditions (pH 7.3, 37 °C).

and COP to those of the nonmodified HSA-FeP2. In contrast, PEG<sub>M5</sub>(HSA-FeP2) showed a higher viscosity and more pronounced hyperoncotic property relative to those of HSA-FeP2. Nevertheless, PEG<sub>M5</sub> conjugate may be useful as an efficient plasma expander (118, 166).

Under physiological conditions, PEG<sub>Mn</sub>(HSA-FeP2) binds and releases O<sub>2</sub>. The  $P_{50}(O_2)$  values were almost identical to those of the original HSA-FeP2, indicating that the O<sub>2</sub> binding equilibrium was not influenced by the presence of the PEG chains (Figure 14b). Surface modification by PEG delays proton-driven oxidation of the O<sub>2</sub> adduct complex, giving HSA-FeP2 the  $\tau_{1/2}(O_2)$  of 12 h, which is almost equal to that of a natural hemoprotein, Mb [ $\tau_{1/2}(O_2)$ , 12 h; pH 7, 35 °C] (167). The conjugated PEG might change the local proton concentration of the HSA interior compared to the outer aqueous solution.

The circulation persistence of FeP2 in the bloodstream was measured after administration of PEG<sub>Mn</sub>(HSA-FeP2) to anesthetized rats (164). The PEG<sub>Mn</sub>(HSA-FeP2) solution (20% volume of the circulatory blood) was injected intravenously into rats from the tail vein. The concentration decays of PEG<sub>Mn</sub>(HSA-FeP2) in the blood showed single exponentials with half-life [ $\tau_{1/2}(FeP2)$ ] of 13–16 h (Figure 14c). These values are considerably longer than those of the corresponding nonmodified HSA-FeP1 (168). Surface modification of HSA-FeP2 by PEG prevented the rapid clearance of the incorporated FeP2. On the basis of these findings, we can conclude that surface modification of HSA-FeP2 by PEG comprehensively improved its O<sub>2</sub> transporting ability.

We then proceeded to evaluate physiological responses to an exchange transfusion with PEG<sub>M2</sub>(HSA-FeP2) in an acute

anemia rat model (169) (Figure 15). The animals were first placed in a 65 vol % hemodilution with 5 g/dL HSA. They subsequently underwent a 30 vol % blood replacement with the PEG<sub>M2</sub>(HSA-FeP2) solution. As negative and positive control groups, a 5 g/dL HSA solution (HSA group) and washed RBC suspension (RBC group) were infused, respectively, to similarly operated rats in hemorrhage. The isovolemic 65% hemodilution with HSA reduced the Hb concentration, thereby decreasing the O<sub>2</sub> supply to the tissue. Consequently, the mean arterial pressure (MAP), renal cortical O<sub>2</sub> partial pressure [PtO<sub>2</sub>(R)], and O<sub>2</sub> partial pressure of muscle tissue [PtO<sub>2</sub>(M)] were decreased. During hemorrhagic shock by 30% bleeding, significant decreases in the MAP, venous O<sub>2</sub> pressure (PvO<sub>2</sub>), PtO<sub>2</sub>(R), and PtO<sub>2</sub>(M) were observed by the loss of the circulation blood volume. The heart rate (HR) and respiration rate were also decreased. In contrast, arterial O<sub>2</sub> pressure (PaO<sub>2</sub>) increased to about 160% of the basal value (b.v.). The arterial CO<sub>2</sub> pressure (PaCO<sub>2</sub>) decreased to about 62% of the b.v.; the pH increased to 7.55.

The injection of the sample solutions increased the blood volume and improved the circulatory flow. Lactate was washed out from the tissues and into the circulatory system, which decreased the pH to the initial level of 7.43 in all groups. The administration of HSA restored no parameters: death occurred within 41 min. In contrast, the infusion of PEG<sub>M2</sub>(HSA-FeP2) or RBC kept all the rats alive until the end of measurements. After injection of PEG<sub>M2</sub>(HSA-FeP2), the animals showed marked and rapid recovery in MAP, HR, PaO<sub>2</sub>, PvO<sub>2</sub>, PaCO<sub>2</sub>, and pH, resembling that shown in the RBC group. These results demonstrate the O<sub>2</sub> transporting capability of the PEG<sub>M2</sub>(HSA-FeP2) solution as a resuscitative fluid. We observed that albumin-based oxygen carrier does not induce hypertensive action, because of its low permeability through the vascular endothelium in comparison with that of Hb molecules. The heart rate responses after the injection were also negligibly small. Visualization of the intestinal microcirculatory changes clearly revealed the widths of the venule and arteriole to be fairly constant (170).

Reversible oxygenation of PEG<sub>M2</sub>(HSA-FeP2) was observed even in the solid state (171). The aqueous solution of PEG<sub>M2</sub>(HSA-FeP2)(CO) complex was spread on the glass plate and dried overnight at room temperature, producing a red transparent solid membrane (Figure 16a). In contrast, HSA-FeP2 without PEG decollation yielded a brittle membrane with many cracks. Scanning electron microscopy (SEM) observations of the PEG<sub>M2</sub>(HSA-FeP2) membrane showed a uniform thickness of 15  $\mu m$  and a smooth surface (Figure 16b). The  $\tau_{1/2}(O_2)$  was 40 h, which is three times longer than the value in water. The

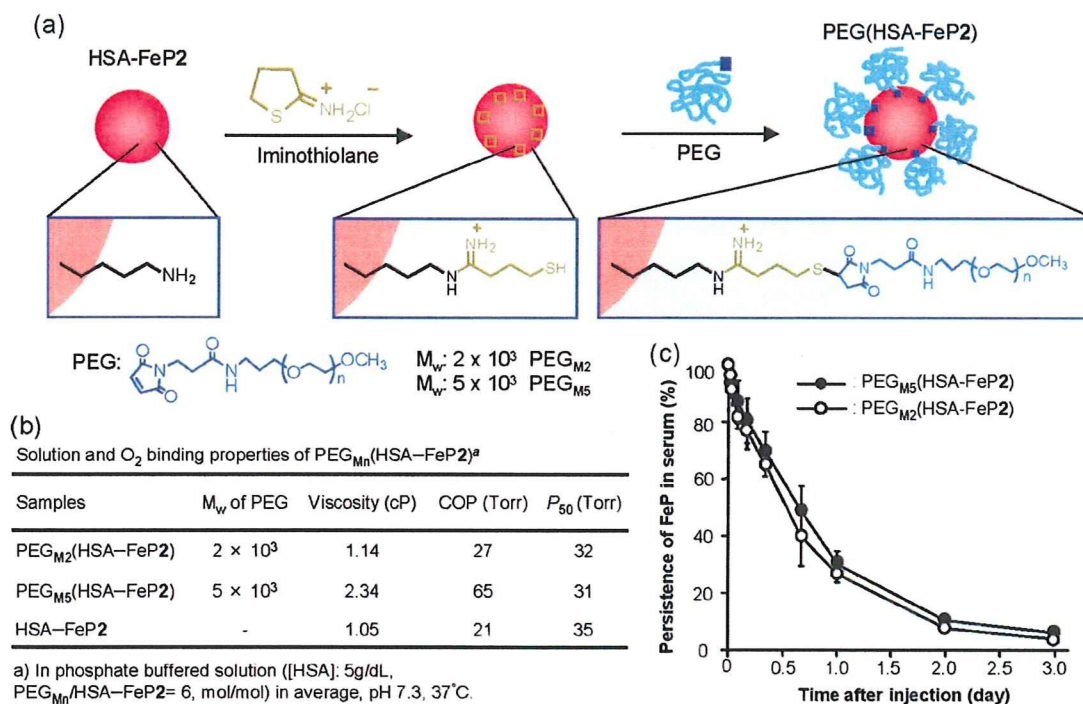


**Figure 14.** Surface modification of HSA-FeP with poly(ethylene glycol). (a) Synthetic scheme of PEG<sub>Mn</sub>(HSA-FeP2). (b) Solution and O<sub>2</sub> binding properties. (c) Persistence of FeP2 in serum after administration of PEG<sub>Mn</sub>(HSA-FeP2) into Wistar rats. Each value represents the mean  $\pm$  SD of four rats.

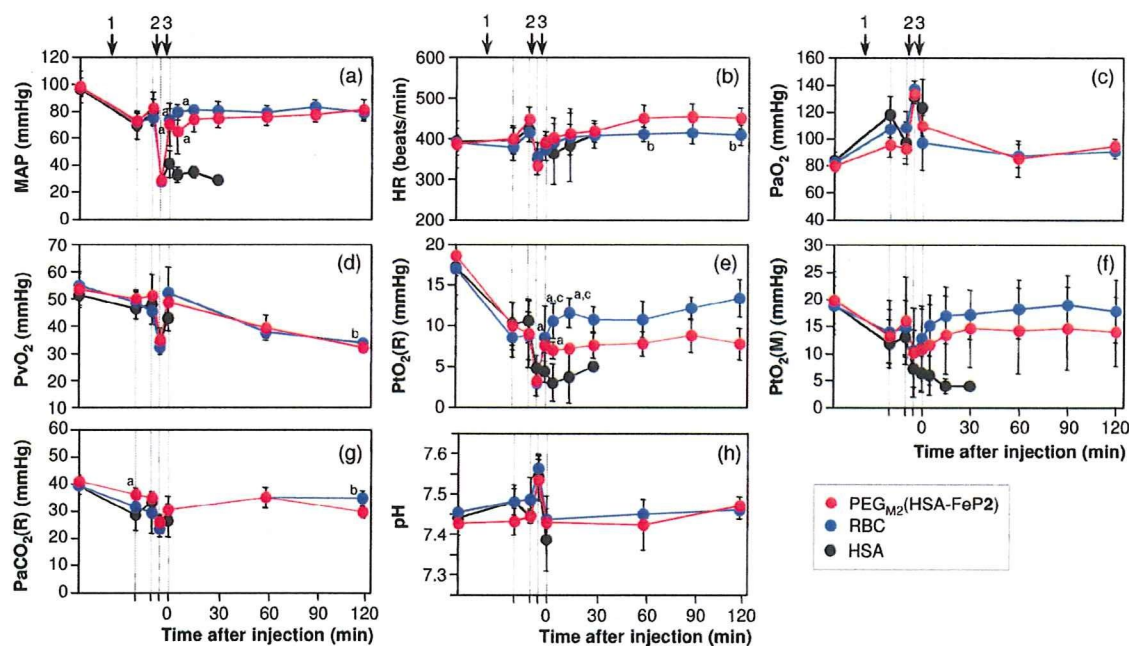


**Figure 15.** Effect of PEG<sub>M2</sub>(HSA-FeP2) solutions on (a) MAP, (b) HR, (c) PaO<sub>2</sub>, (d) PvO<sub>2</sub>, (e) PtO<sub>2</sub>(R), (f) PtO<sub>2</sub>(M), (g) PaCO<sub>2</sub>, and (h) pH in anesthetized rats subjected to hemodilution and hemorrhage. Each value represents the mean  $\pm$  SD of five rats [red, PEG<sub>M2</sub>(HSA-FeP2) group; blue, washed RBC group; and black, HSA group]. Arrows (1), (2), and (3), respectively, indicate the periods of 65% hemodilution, 30% bleeding, and sample infusion. <sup>a</sup> $p < 0.05$  versus HSA group (Tukey-Kramer test), <sup>b</sup> $p < 0.05$  versus PEG<sub>M2</sub>(HSA-FeP2) group (unpaired *t*-test), and <sup>c</sup> $p < 0.05$  versus PEG<sub>M2</sub>(HSA-FeP2) group (Tukey-Kramer test).

O<sub>2</sub> binding affinity was about a half that of the monomeric PEG<sub>M2</sub>(HSA-FeP2).

We subsequently added hyaluronic acid (HA) as a supporting polymer to the protein solution and prepared the solid membrane on a poly(styrene) dish. Actually, HA is known as a glycosaminoglycan component of connective tissues, hyaline bodies, and extracellular matrix (172). Water evaporation of the PEG<sub>M2</sub>(HSA-FeP2)/HA mixture ([HSA]: 2.5 wt % and [HA]: 0.2 wt %)

produced a uniform red solid membrane that was easily peeled from the dish, yielding a free-standing homogeneous thin film of the PEG(HSA-FeP2)/HA hybrid (Figure 16c,d).

The PEG<sub>M2</sub>(HSA-FeP2) solution is useful as a valuable O<sub>2</sub>-carrying plasma. Membranes of PEG<sub>M2</sub>(HSA-FeP2) with micrometer thickness can serve as a RBC substitute that can be preserved anywhere and reproduced as a saline solution at any time.

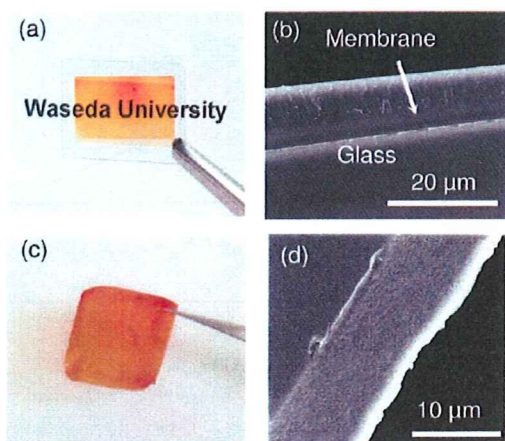


**Figure 16.** The solid membrane of PEG<sub>M2</sub>(HSA-FeP). (a) Photograph of the membrane on the glass, (b) SEM of the membrane section, (c) photograph of the flexible film peeled from the poly(styrene) dish, and (d) SEM of the isolated film.

### 3.3. Recombinant HSA-Heme (rHSA-Heme) Prepared Using Site-Directed Mutagenesis.

Hemin [Fe<sup>3+</sup>protoporphyrin IX] released from methHb during enucleation of RBC or through hemolysis is captured by HSA with a high binding constant ( $K \approx 10^8 \text{ M}^{-1}$ ) (173). Crystallographic studies have revealed that hemin is bound within a narrow D-shaped hydrophobic cavity in subdomain IB with axial coordination of Tyr-161 to the central ferric ion and electrostatic interactions between the porphyrin propionates and a triad of basic amino acid residues (Arg-114, His-146, and Lys-190) (Figure 17) (174, 175). In terms of the general hydrophobicity of this  $\alpha$ -helical heme pocket, the subdomain IB of HSA potentially has similar features to the heme binding site of Hb or Mb. However, when one reduces HSA-hemin to obtain the ferrous complex, it is autoxidized rapidly by O<sub>2</sub>, even at low temperature ( $\sim 0^\circ \text{C}$ ), because HSA lacks the proximal His, which, in Hb and Mb, enables the prosthetic heme group to bind O<sub>2</sub>. Knowledge of the detailed architecture of the heme binding site in HSA enables us to design mutagenesis experiments to construct a tailor-made heme pocket for stable O<sub>2</sub> binding. Therefore, we used site-directed mutagenesis to introduce an His into the heme binding site that was expected to provide axial coordination to the central Fe<sup>2+</sup> atom of the heme and thereby promote O<sub>2</sub> binding.

Results of our modeling experiments suggested that a favorable position for the axial imidazole insertion would be Ile-142 (Figure 17). The N<sub>ε</sub>(His)-Fe distances were estimated as 2.31 Å for H142 (compared to 2.18 Å for Mb). We therefore designed and produced two single mutants I142H and a double mutant I142H/Y161L (HL) (176).

In the UV-vis absorption spectrum of rHSA(HL)-hemin, the ligand-to-metal charge transfer band at 625 nm was weakened because of the Y161L mutation. The MCD spectrum of rHSA(HL)-hemin showed a similar S-shaped pattern in the Soret band region resembling that of ferric Mb (177, 178). These results suggest that rHSA(HL)-hemin is in a predominantly ferric high-spin complex having a water molecule as the sixth ligand. The rHSA-hemin was easily reduced to the ferrous complex by adding a small molar excess of aqueous sodium dithionite under an Ar atmosphere (Figure 18). A single broad absorption band ( $\lambda_{\text{max}}$ : 559 nm) in the visible absorption spectrum and the MCD spectrum of rHSA(HL)-heme indicated the formation of a five-N-coordinate high-spin complex (176, 177, 179). The heme therefore appears to be accommodated in the mutated heme pocket with an axial coordination involving His-142. Upon exposure of rHSA(HL)-heme solution to O<sub>2</sub>, the UV-vis absorption changed immediately to that of the O<sub>2</sub> adduct

complex (Figure 18). It formed a carbonyl complex under a CO atmosphere. The single mutant rHSA(I142H)-heme, which retains Y161, was unable to bind O<sub>2</sub>. The polar phenolate residue at the top of the porphyrin plane is likely to accelerate the proton-driven oxidation of the Fe<sup>2+</sup> center. The replacement of Tyr-161 in rHSA(I142H)-heme by Leu enhanced stabilization of the O<sub>2</sub> adduct complex.

To evaluate the kinetics of O<sub>2</sub> and CO bindings to rHSA-hemes, laser flash photolysis experiments were carried out (Tables 7 and 8). It is noteworthy that the absorbance decay accompanying the CO recombination to rHSA(HL)-heme was composed of double-exponential profiles, which is normally not observed in Mb (the faster phase is defined as species I; the slower phase is defined as species II). The ratio of the amplitude of the species I and the species II was approximately 3:2. On the other hand, the rebinding of O<sub>2</sub> to rHSA(HL)-heme followed a simple monophasic decay. Numerous investigations of synthetic model hemes have helped to reveal the relation between the structure around the hemes and their O<sub>2</sub> and CO binding abilities (4, 147, 148). A bending strain in the proximal base coordination to the central Fe<sup>2+</sup> atom, the "proximal-side steric (proximal pull) effect", is known to be capable of both increasing the dissociation rate for CO and decreasing the association rate. Simultaneously, it increases the O<sub>2</sub> dissociation rate without greatly altering the O<sub>2</sub> association kinetics. Consequently, one possible explanation for the existence of the two phases is that two different geometries of the axial His (His-142) coordination to the central ferrous ion of the heme might exist, each one accounting for a component of the biphasic kinetics of CO rebinding.

### 3.4. Modulation of O<sub>2</sub> Binding Property of rHSA-(mutant)-Heme.

To control the O<sub>2</sub> binding affinity of rHSA-heme, we designed and produced diverse rHSA(mutant)-hemes in which bulky hydrophobic or hydrophilic amino acids were introduced around the O<sub>2</sub> binding site (Tyr-161, Leu-182, Leu-185, and Arg-186) (Figure 17). More recently, the beneficial effect of low-dose CO on the microcirculation by a hemoglobin-based artificial oxygen carrier has been discussed (132, 182). Control of the CO binding affinity of rHSA-heme is also tempting.

**A. Substitution of Tyr-161 with Leu or Phe.** The first, Tyr-161, was substituted to noncoordinating and hydrophobic amino acids (Leu or Phe). The O<sub>2</sub> and CO binding properties of rHSA(HL)-heme and rHSA(I142H/Y161F)-heme [rHSA(HF)-heme] showed that the presence of a Phe rather than a Leu at position 161 results in 6-fold and 4-fold increases in the O<sub>2</sub> binding affinity for species I and II, respectively (Table 7). This enhancement is mainly attributable to an increase in the O<sub>2</sub> association rate constant. The same trend was observed for CO binding [3-fold increase in  $k_{\text{on}}(\text{CO})$ ] (Table 8). The substitution of Leu-161 (102 Å<sup>3</sup>) by Phe-161 (137 Å<sup>3</sup>) (183) replaces an isopropyl group with a rigid benzyl group within the heme pocket. In rHSA(HL), the small side chain of Leu-161 might enable free rotation of the side chain of neighboring Leu-185, thereby reducing the volume on the distal side of the porphyrin plane (Figure 19a,b). On the other hand, the bulkier aromatic side chain of Phe-161 might prevent rotation of the isopropyl group of Leu-185 and thereby provide greater room of the distal pocket; this effect might provide easier access to the heme Fe<sup>2+</sup> atom and account for the increased association rates for O<sub>2</sub> and CO.

**B. Substitution of Leu-185 with Polar Amino Acid.** Leu-185 was substituted with a more hydrophilic amino acid (Asn, Gln, or His), which was expected to interact with the coordinated O<sub>2</sub> by hydrogen bond and to stabilize the O<sub>2</sub> adduct complex similarly to Hb and Mb. In rHSA(mutant)-hemes in which Gln or His was introduced into Leu-185, they formed ferrous six-coordinated low-spin complexes under an Ar atmosphere. That

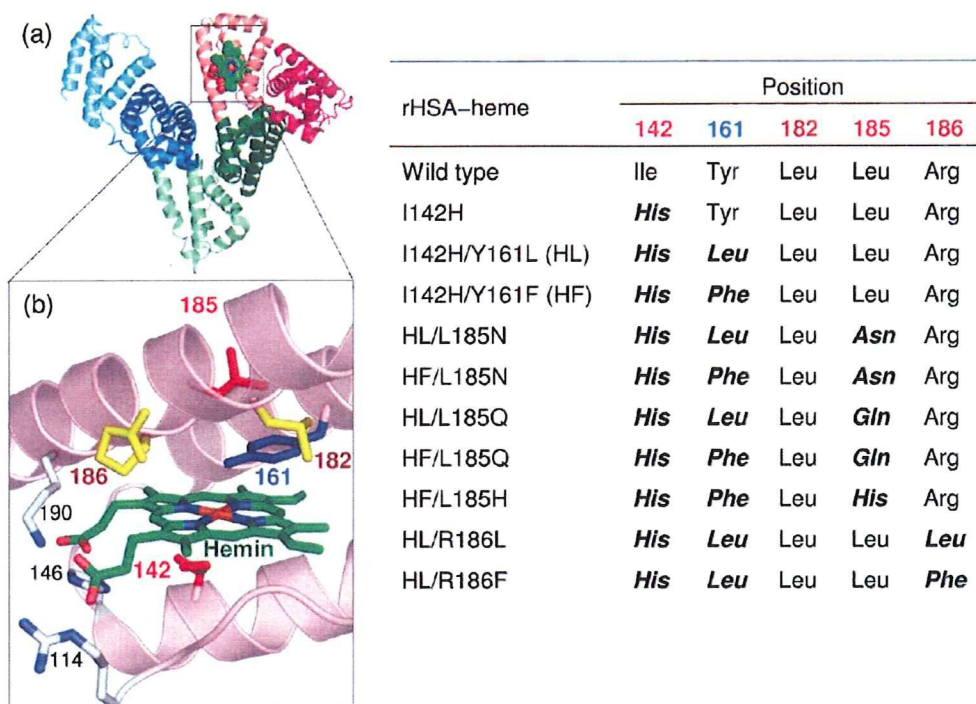


**Figure 17.** (a) Crystal structure of HSA-hemin complex (1O9X) from ref 174. Hemin is shown in a space-filling representation. (b) Heme pocket structure in subdomain IB and positions of amino acids where site-specific mutations were introduced. Abbreviations of rHSA(mutant)s are shown in the table.

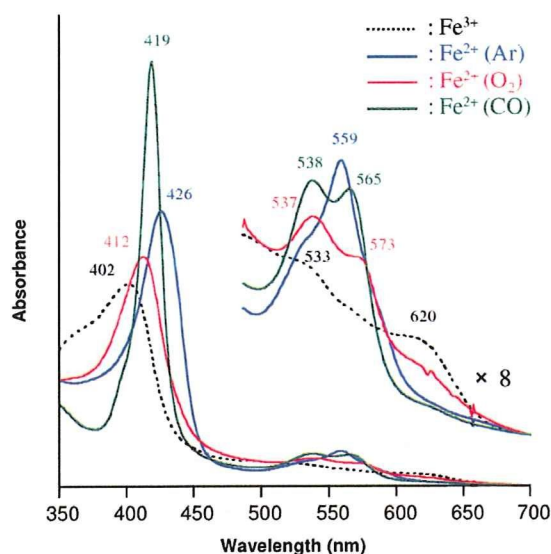


**Figure 18.** UV-vis absorption spectral changes of rHSA(HL)-heme in potassium phosphate buffered solution (pH 7.0).

result suggests that the introduced amino acid coordinates to the heme iron as a sixth ligand under an Ar atmosphere. Upon exposure of the solutions to O<sub>2</sub>, they were oxidized. Bis-histidyl hemochromes are known to be oxidized by O<sub>2</sub> rapidly via an outer sphere mechanism (184–186). On the other hand, rHSA(HL/L185N)-heme and rHSA(HF/L185N)-heme in which Asn was introduced at Leu-185 formed ferrous five-coordinated high-spin complexes under an Ar atmosphere. They formed O<sub>2</sub> adduct complexes under O<sub>2</sub> atmosphere. The introduced Asn is estimated to be too far to coordinate to the heme.

Marked differences were apparent in a comparison of the O<sub>2</sub> and CO binding parameters for rHSA(HL)-heme and rHSA(HL/L185N)-heme. First, the presence of Asn rather than Leu at

**Table 7.** O<sub>2</sub> Binding Parameters of rHSA(Mutant)-Heme Complexes in Phosphate Buffered Solution (pH 7.0) at 22 °C

hemoproteins	$k_{on}(O_2)$ ( $\mu M^{-1}s^{-1}$ )	$k_{off}(O_2)$ (m s <sup>-1</sup> )		$P_{50}(O_2)$ (Torr)	
		I	II	I	II
rHSA(HL)-heme	7.5	0.22	1.70	18	134
rHSA(HF)-heme	20	0.10	0.99	3	31
rHSA(HL/L185N)-heme	14	0.02	0.29	1	14
rHSA(HF/L185N)-heme	26	0.10	1.03	2	24
rHSA(HL/R186L)-heme	25	0.41	8.59	10	209
rHSA(HL/R186F)-heme	21	0.29	7.01	9	203
Mb <sup>a</sup>	14	0.012		0.51	
RBC <sup>b</sup>				8	

<sup>a</sup> Sperm whale myoglobin in 0.1 M potassium phosphate buffer (pH 7.0, 20 °C); ref 180. <sup>b</sup> Human red cell suspension in isotonic buffer (pH 7.4, 20 °C); ref 181.

**Table 8.** CO Binding Parameters of rHSA(Mutant)-Heme Complexes in Phosphate Buffered Solution (pH 7.0) at 22 °C

hemoproteins	$k_{on}(CO)$ ( $\mu M^{-1}s^{-1}$ )		$k_{off}(CO)$ (s <sup>-1</sup> )		$P_{50}(CO)$ (Torr)	
	I	II	I	II	I	II
rHSA(HL)-heme	2.0	0.27	0.013	0.079	0.0053	0.240
rHSA(HF)-heme	6.8	0.72	0.009	0.061	0.0011	0.068
rHSA(HL/L185N)-heme	6.8	1.60	0.008	0.039	0.0010	0.020
rHSA(HF/L185N)-heme	7.7	1.09	0.008	0.043	0.0008	0.032
rHSA(HL/R186L)-heme	5.0	0.57	0.011	0.165	0.0018	0.234
rHSA(HL/R186F)-heme	7.9	1.12	0.010	0.148	0.0010	0.107
Mb <sup>a</sup>	0.51		0.019		0.03	

<sup>a</sup> Sperm whale myoglobin in 0.1 M potassium phosphate buffer (pH 7.0, 20 °C); ref 180.

position 185 caused 2-fold and 3–6-fold increases, respectively, in the  $k_{on}(O_2)$  and  $k_{on}(CO)$  values. The Asn might partly rotate upward, which provides somewhat greater space of the distal pocket. Second, Asn-185 induced 18-fold and 10-fold increases in the O<sub>2</sub> binding affinity for species I and II, because the  $k_{off}(O_2)$

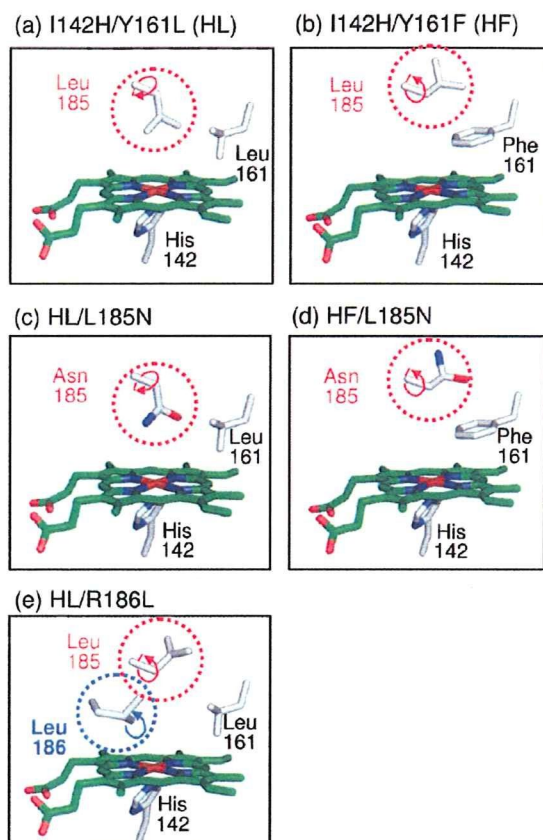


**Figure 19.** The proposed configuration of Leu-185 in (a) rHSA(HL)-heme and (b) rHSA(HF)-heme, Asn-185 in (c) rHSA(HL/L185N)-heme and (d) rHSA(HF/L185N)-heme, and Leu-186 in (e) rHSA(HL/R186L)-heme.

values were 1/6–1/11 of their former values. This corresponds to a free energy difference of  $-1.8 \text{ kcal mol}^{-1}$  at  $22 \text{ }^\circ\text{C}$ . The magnitude of the effect seems to be reasonable considering that, in  $\text{HbO}_2$  and  $\text{MbO}_2$ , the distal His-64 stabilizes the coordinated  $\text{O}_2$  by  $-0.6$  to  $-1.4 \text{ kcal mol}^{-1}$  because of the hydrogen bond (187). In contrast, the  $\text{O}_2$  and CO binding parameters for rHSA(HF)-heme and rHSA(HF/L185N)-heme showed no significant differences. The bulky benzyl side chain of Phe-161 can prevent rotation of the polar amide group of Asn-185 and thereby decrease the effect of polarity and size on  $\text{O}_2$  and CO binding parameters (Figure 19c,d) (188).

**C. Substitution of Arg-186 with Leu or Phe.** For administration into the human circulatory system, it would be better if the affinity were similar to the human RBC [ $P_{50}(\text{O}_2)$ : 8 Torr,  $25 \text{ }^\circ\text{C}$ ]. It is expected that providing a certain degree of hydrophobicity into the distal side of the heme by insertion of a nonpolar residue would reduce the  $\text{O}_2$  binding affinity of the rHSA-heme complex. The most suitable position for that introduction might be at Arg-186, which is the entrance of the heme pocket and which is rather close to the central Fe(II) ion. Therefore, rHSA(HL/R186L)-hemin and rHSA(HL/R186F)-hemin were prepared. The  $\text{O}_2$  dissociation rate constants of rHSA(HL/R186L)-heme and rHSA(HL/R186F)-heme were 3–4-fold higher than that of rHSA(HF)-heme, which reduced the  $\text{O}_2$  binding affinities [larger  $P_{50}(\text{O}_2)$ ]. This reduction might be attributable to the increased hydrophobicity in the distal pocket. The  $\text{O}_2$  binding affinities of rHSA(HL/R186L)-heme [ $P_{50}(\text{O}_2)$ : 10 Torr] and rHSA(HL/R186F)-heme [ $P_{50}(\text{O}_2)$ : 9 Torr] have become equivalent to those of human RBC. The important structural factor in these mutants is Y161L, which enables the rotation of the isopropyl group of Leu-185 above

the  $\text{O}_2$  coordination site. Unexpectedly, the  $k_{\text{on}}(\text{O}_2)$  and  $k_{\text{on}}(\text{CO})$  values of rHSA(HL/R186L)-heme and rHSA(HL/R186F)-heme were 3-fold and 3–4-fold higher than those of rHSA(HL)-heme and in the same range as that of rHSA(HF)-heme. In fact, Leu-161 is small, but the hydrophobic Leu-186 or Phe-186 might be integrated into the heme pocket from the entrance and might push up the neighboring Leu-185 residue (Figure 19e) (188).

We have engineered mutant rHSA-heme complexes that can bind  $\text{O}_2$ . Principal modifications to the heme pocket that are necessary to confer reversible  $\text{O}_2$  binding are (i) replacement of Tyr-161 by hydrophobic amino acid (Leu or Phe), and (ii) introduction of His as a proximal base at position Ile-142. Furthermore, (iii) modification of the distal amino acid has a considerable effect on the modulation of  $\text{O}_2$  and CO binding affinities.

#### 4. CONCLUSIONS

The structures of our artificial  $\text{O}_2$  carriers differ greatly from those of sophisticated RBCs. However, clear advantages of simplified artificial  $\text{O}_2$  carriers are readily apparent: the absence of blood-type antigens and infectious viruses, stability for long-term storage at room temperature for any emergency, all of which overwhelm the functionality of RBCs. The shorter half-life of artificial  $\text{O}_2$  carriers in the bloodstream (ca. 3 days) limits their use, but they are applicable as a transfusion alternative for shorter periods of use. Easy manipulation of physicochemical properties such as  $P_{50}(\text{O}_2)$  and viscosity supports their possible development of tailor-made  $\text{O}_2$  carriers to suit various clinical indications. The achievements of ongoing research described above give us confidence in advancing the further development with the expectation of its eventual realization.

#### ACKNOWLEDGMENT

The authors gratefully acknowledge Prof. H. Nishide, Prof. S. Takeoka (Waseda Univ.), Prof. R. Yozu, Prof. M. Suematsu, Dr. H. Horinouchi, Dr. M. Watanabe, Dr. E. Ikeda, Dr. Y. Izumi, Dr. M. Yamamoto, Dr. T. Ikeda (Keio Univ.), Dr. H. Ikeda, Dr. H. Azuma, Dr. M. Fujiwara, Dr. H. Abe (Hokkaido Red Cross Blood Center), Dr. M. Takaori (East Takarazuka Satoh Hospital), Prof. M. Otagiri (Kumamoto Univ.), Prof. M. Intaglietta (Univ. of California, San Diego), Prof. W. T. Phillips (Univ. of Texas, San Antonio), Prof. D. Erni (Inselspital Hospital, Univ. of Berne), Prof. M. Okamoto (Weill Med. College, Cornell Univ.), Prof. S. Curry (Imperial College London) and their active colleagues for meaningful discussions and contributions to this research. This work was partly supported by Health Sciences Research Grants (Research on Regulatory Science) from the Ministry of Health, Labour and Welfare, Japan, and Grant-in-Aid for Scientific Research from JSPS. The authors are the holders of patents related to the production and utilization of HbV and albumin-hemes.

#### LITERATURE CITED

- (1) Perutz, M. F. (1970) Stereochemistry of cooperative effects in haemoglobin. *Nature* 228, 726–739.
- (2) Jones, R. D., Summerville, A., and Basolo, F. (1979) Synthetic oxygen carriers related to biological systems. *Chem. Rev.* 79, 139–179.
- (3) Collman, J. P. (1977) Synthetic model for the oxygen-binding hemoproteins. *Acc. Chem. Res.* 10, 265–272.
- (4) Momenteau, M., and Reed, C. (1994) Synthetic heme dioxygen complexes. *Chem. Rev.* 94, 659–698.
- (5) Collman, J. P., Gagne, R. R., Halbert, T. R., Marchon, J.-C., and Reed, C. A. (1973) Reversible oxygen adduct formation in ferrous complexes derived from "picket fence" porphyrins. A model for oxymyoglobin. *J. Am. Chem. Soc.* 73, 7868–7870.

- (6) Collman, J. P., Gagne, R. R., Reed, C. A., Halbert, T. R., Lang, G., and Robinson, W. T. (1975) "Picket fence porphyrins." Synthetic models for oxygen binding hemoproteins. *J. Am. Chem. Soc.* 97, 1427–1439.
- (7) Matsushita, Y., Hasegawa, E., Eshima, K., and Tsuchida, E. (1983) Synthesis of amphiphilic porphyratoiron complexes having phosphocholine groups. *Chem. Lett.* 1983, 1387–1389.
- (8) Tsuchida, E. (1985) Liposome-embedded iron-porphyrins as an artificial oxygen carrier. *Ann. N.Y. Acad. Sci.* 446, 429–442.
- (9) Tsuchida, E., and Nishide, H. (1986) Hemoglobin model - artificial oxygen carrier composed of porphyratoiron complexes. *Top. Curr. Chem.* 1132, 63–99.
- (10) Komatsu, T., Moritake, M., Nakagawa, A., and Tsuchida, E. (2002) Self-organized lipid-porphyrin bilayer membranes in vesicular form: nanostructure, photophysical properties and dioxygen coordination. *Chem. Eur. J.* 8, 5469–5480.
- (11) Komatsu, T., Ando, K., Kawai, N., Nishide, H., and Tsuchida, E. (1995) O<sub>2</sub>-transport albumin - a new hybrid hemoprotein incorporating tetraphenylporphyratoiron(II). *Chem. Lett.* 813–814.
- (12) Savitsky, J. P., Doczi, J., Black, J., and Arnold, J. D. (1978) A clinical safety trial of stroma-free hemoglobin. *Clin. Pharm. Ther.* 23, 73–80.
- (13) Greenwald, R. B., Pendri, A., Martinez, A., Gilbert, C., and Bradley, P. (1996) PEG thiazolidine-2-thione, a novel reagent for facile protein modification: conjugation of bovine hemoglobin. *Bioconjugate Chem.* 7, 638–641.
- (14) Kluger, R., and Li, X. (1997) Efficient chemical introduction of a disulfide cross-link and conjugation site into human hemoglobin at  $\beta$ -lysine-82 utilizing a bifunctional aminoacyl phosphate. *Bioconjugate Chem.* 8, 921–926.
- (15) Sakai, H., Yuasa, M., Onuma, H., Takeoka, S., and Tsuchida, E. (2000) Synthesis and physicochemical characterization of a series of hemoglobin-based oxygen carriers: objective comparison between cellular and acellular types. *Bioconjugate Chem.* 11, 56–64.
- (16) Hai, T. T., Pereira, D. E., Nelson, D. J., Catarello, J., and Smak, A. (2000) Surface modification of diaspirin cross-linked hemoglobin (DCLHb) with chondroitin-4-sulfate derivatives. Part 1. *Bioconjugate Chem.* 11, 705–713.
- (17) Manjula, B. N., Tsai, A., Upadhyaya, R., Perumalsamy, K., Smith, P. K., Malavalli, A., Vandegriff, K., Winslow, R. M., Intaglietta, M., Prabhakaran, M., Friedman, J. M., and Acharya, A. S. (2003) Site-specific PEGylation of hemoglobin at Cys-93( $\beta$ ): correlation between the colligative properties of the PEGylated protein and the length of the conjugated PEG chain. *Bioconjugate Chem.* 14, 464–472.
- (18) Murray, J. A., Ledlow, A., Launsbach, J., Evans, D., Loveday, M., and Conklin, J. L. (1995) The effects of recombinant human hemoglobin on esophageal motor function in humans. *Gastroenterology* 109, 1241–1248.
- (19) Chatterjee, R., Welty, E. V., Walder, R. Y., Pruitt, S. L., Rogers, S. L., Arnone, A., and Walder, J. A. (1986) Isolation and characterization of a new hemoglobin derivative cross-linked between the  $\alpha$  chains (lysine 99 $\alpha_1$   $\gg$  lysine 99 $\alpha_2$ ). *J. Biol. Chem.* 261, 9929–9937.
- (20) Iwashita, Y. (1991) Pyridoxalated hemoglobin-polyoxyethylene conjugate (PHP) as an O<sub>2</sub> carrier. *Artif. Organs Today* 1, 89–114.
- (21) Riess, J. G. (2001) Oxygen carriers ("blood substitutes") - raison d'être, chemistry, and some physiology. *Chem. Rev.* 101, 2797–2920.
- (22) de Figueiredo, L. F., Mathru, M., Solanki, D., Macdonald, V. W., Hess, J., and Kramer, G. C. (1997) Pulmonary hypertension and systemic vasoconstriction might offset the benefits of acellular hemoglobin blood substitutes. *J. Trauma* 42, 847–854.
- (23) Tsai, A. G., Kerger, H., and Intaglietta, M. (1995) Microcirculatory consequences of blood substitution with  $\alpha\alpha$ -hemoglobin. In *Blood Substitutes: Physiological Basis of Efficacy* (Winslow, R. M., Vandegriff, K., Intaglietta, M., Eds.) pp155–174, Birkhauser, Boston.
- (24) Goda, N., Suzuki, K., Naito, M., Takeoka, S., Tsuchida, E., Ishimura, Y., Tamatani, T., and Suematsu, M. (1998) Distribution of heme oxygenase isoforms in rat liver. Topographic basis for carbon monoxide-mediated microvascular relaxation. *J. Clin. Invest.* 101, 604–612.
- (25) Sakai, H., Hara, H., Yuasa, M., Tsai, A. G., Takeoka, S., Tsuchida, E., and Intaglietta, M. (2000) Molecular dimensions of Hb-based O<sub>2</sub> carriers determine constriction of resistance arteries and hypertension. *Am. J. Physiol. Heart Circ. Physiol.* 279, H908–H915.
- (26) Burhop, K., Gordon, D., and Estep, T. (2004) Review of hemoglobin-induced myocardial lesions. *Artif. Cells Blood Substit. Immobil. Biotechnol.* 32, 353–374.
- (27) Neragi-Miandoab, S., and Vlahakes, G. J. (2006) Elevated troponin I level with hemoglobin based oxygen carrying solutions (HBOCs) as a priming solution despite improved left ventricular function. *Interact. Cardiovasc. Thorac. Surg.* 5, 135–138.
- (28) Natanson, C., Kern, S. J., Lurie, P., Banks, S. M., and Wolfe, S. M. (2008) Cell-free hemoglobin-based blood substitutes and risk of myocardial infarction and death: a meta-analysis. *JAMA* 299, 2304–2312.
- (29) Balla, J., Jacob, H. S., Balla, G., Nath, K., Eaton, J. W., and Vercellotti, G. M. (1993) Endothelial-cell heme uptake from heme proteins: induction of sensitization and desensitization to oxidant damage. *Proc. Natl. Acad. Sci. U.S.A.* 90, 9285–9289.
- (30) Sakai, H., Sato, A., Masuda, K., Takeoka, S., and Tsuchida, E. (2008) Encapsulation of concentrated hemoglobin solution in phospholipid vesicles retards the reaction with NO, but not CO, by intracellular diffusion barrier. *J. Biol. Chem.* 283, 1508–1517.
- (31) Sakai, H., Sato, A., Sobolewski, P., Takeoka, S., Frangos, J. A., Kobayashi, K., Intaglietta, M., and Tsuchida, E. (2008) NO and CO binding profiles of hemoglobin vesicles as artificial oxygen carriers. *Biochim. Biophys. Acta* 1784, 1441–1447.
- (32) Martini, J., Cabrales, P., Tsai, A. G., and Intaglietta, M. (2006) Mechanotransduction and the homeostatic significance of maintaining blood viscosity in hypotension, hypertension and haemorrhage. *J. Intern. Med.* 259, 364–372.
- (33) Sakai, H., Suzuki, Y., Kinoshita, M., Takeoka, S., Maeda, N., and Tsuchida, E. (2003) O<sub>2</sub> release from Hb vesicles evaluated using an artificial, narrow O<sub>2</sub>-permeable tube: comparison with RBCs and acellular Hbs. *Am. J. Physiol. Heart Circ. Physiol.* 285, H2543–H2555.
- (34) Vandegriff, K. D., and Olson, J. S. (1984) The kinetics of O<sub>2</sub> release by human red blood cells in the presence of external sodium dithionite. *J. Biol. Chem.* 259, 12609–12618.
- (35) Chang, T. M. S. (2005) Therapeutic applications of polymeric artificial cells. *Nat. Rev. Drug Discov.* 4, 221–235.
- (36) Toyoda, T. (1965) Artificial blood. *Kagaku* 35, 7–13 (in Japanese).
- (37) Kimoto, S., Hori, M., Toyoda, T., and Sekiguchi, W. (1968) Artificial red cells. *Gekachiryō (Surgical Therapy)* 19, 324–332 (in Japanese).
- (38) Bangham, A. D., and Horne, R. W. (1964) Negative staining of phospholipids and their structure modification by surface-active agents as observed in the electron microscope. *J. Mol. Biol.* 8, 660–668.
- (39) Bangham, A. D., Standish, M. M., and Watkins, J. C. (1965) Diffusion of univalent ions across the lamellae of swollen phospholipids. *J. Mol. Biol.* 13, 238–252.
- (40) Djordjevich, L., and Miller, I. F. (1977) Lipid encapsulated hemoglobin as a synthetic erythrocyte. *Fed. Proc.* 36, 567–571.
- (41) Farmer, M. C., Rudolph, A. S., Vandegriff, K. D., Hayre, M. D., Bayne, S. A., and Johnson, S. A. (1988) Liposome-encapsulated hemoglobin: oxygen binding properties and respiratory function. *Biomater. Artif. Cells Artif. Organs* 16, 289–299.
- (42) Rudolph, A. S., Klipper, R. W., Goins, B., and Phillips, W. T. (1991) In vivo biodistribution of a radiolabeled blood substitute: <sup>99m</sup>Tc-labeled liposome-encapsulated hemoglobin in an anesthetized rabbit. *Proc. Natl. Acad. Sci. U.S.A.* 88, 10976–10980.

- (43) Phillips, W. T., Klipper, R. W., Awasthi, V. D., Rudolph, A. S., Cliff, R., Kwasiborski, V., and Goins, B. A. (1999) Polyethylene glycol-modified liposome-encapsulated hemoglobin: a long circulating red cell substitute. *J. Pharmacol. Exp. Ther.* 288, 665–670.
- (44) Usuba, A., Osuka, F., Kimura, T., Sato, R., Ogata, Y., Gotoh, H., Kimura, T., and Fukui, H. (1998) Effect of liposome-encapsulated hemoglobin, neo red cells, on hemorrhagic shock. *Surg. Today* 28, 1027–1035.
- (45) Yoshioka, H. (1991) Surface modification of haemoglobin-containing liposomes with polyethylene glycol prevents liposome aggregation in blood plasma. *Biomaterials* 12, 861–864.
- (46) Sakai, H., Hamada, K., Takeoka, S., Nishide, H., and Tsuchida, E. (1996) Physical properties of hemoglobin vesicles as red cell substitutes. *Biotechnol. Prog.* 12, 119–125.
- (47) Takeoka, S., Ohgushi, T., Terasa, K., Ohmori, T., and Tsuchida, E. (1996) Layer-controlled hemoglobin vesicles by interaction of hemoglobin with a phospholipid assembly. *Langmuir* 12, 1755–1759.
- (48) Sou, K., Naito, Y., Endo, T., Takeoka, S., and Tsuchida, E. (2003) Effective encapsulation of proteins into size-controlled phospholipid vesicles using freeze-thawing and extrusion. *Biotechnol. Prog.* 19, 1547–1552.
- (49) Sakai, H., Takeoka, S., Yokohama, H., Seino, Y., Nishide, H., and Tsuchida, E. (1993) Purification of concentrated Hb using organic solvent and heat treatment. *Protein Expression Purif.* 4, 563–569.
- (50) Abe, H., Ikebuchi, K., Hirayama, J., Fujihara, M., Takeoka, S., Sakai, H., Tsuchida, E., and Ikeda, H. (2001) Virus inactivation in hemoglobin solution by heat treatment. *Artif. Cells Blood Substit. Immobil. Biotechnol.* 29, 381–388.
- (51) Chung, J., Hamada, K., Sakai, H., Takeoka, S., and Tsuchida, E. (1995) Ligand-exchange reaction of carbonylhemoglobin to oxyhemoglobin in a hemoglobin liquid membrane. *Nippon Kagaku Kaishi* 2, 123–127 (in Japanese).
- (52) Takeoka, S., Sakai, H., Kose, T., Mano, Y., Seino, Y., Nishide, H., and Tsuchida, E. (1997) Methemoglobin formation in hemoglobin vesicles and reduction by encapsulated thiols. *Bioconjugate Chem.* 8, 539–544.
- (53) Teramura, Y., Kanazawa, H., Sakai, H., Takeoka, S., and Tsuchida, E. (2003) Prolonged oxygen-carrying ability of hemoglobin vesicles by coencapsulation of catalase *in vivo*. *Bioconjugate Chem.* 14, 1171–1176.
- (54) Sakai, H., Masada, Y., Onuma, H., Takeoka, S., and Tsuchida, E. (2004) Reduction of methemoglobin via electron transfer from photoreduced flavin: restoration of O<sub>2</sub>-binding of concentrated hemoglobin solution coencapsulated in phospholipid vesicles. *Bioconjugate Chem.* 15, 1037–1045.
- (55) Atoji, T., Aihara, M., Sakai, H., Tsuchida, E., and Takeoka, S. (2006) Hemoglobin vesicles containing methemoglobin and L-tyrosine to suppress methemoglobin formation *in vitro* and *in vivo*. *Bioconjugate Chem.* 17, 1241–1245.
- (56) Sakai, H., Takeoka, S., Seino, Y., and Tsuchida, E. (1994) Suppression of methemoglobin formation by glutathione in a concentrated hemoglobin solution and in a Hb-vesicle. *Bull. Chem. Soc. Jpn.* 67, 1120–1125.
- (57) Rameez, S., Alost, H., and Palmer, A. F. (2008) Biocompatible and biodegradable polymersome encapsulated hemoglobin: a potential oxygen carrier. *Bioconjugate Chem.* 19, 1025–1032.
- (58) Zhao, J., Liu, C. S., Yuan, Y., Tao, X. Y., Shan, X. Q., Sheng, Y., and Wu, F. (2007) Preparation of hemoglobin-loaded nanosized particles with porous structure as oxygen carriers. *Biomaterials* 28, 1414–1422.
- (59) Rudolph, A. S. (1988) The freeze-dried preservation of liposome encapsulated hemoglobin: a potential blood substitute. *Cryobiology* 25, 277–284.
- (60) Rabinovici, R., Rudolph, A. S., Vernick, J., and Feuerstein, G. (1994) Lyophilized liposome encapsulated hemoglobin: evaluation of hemodynamic, biochemical, and hematologic responses. *Crit. Care Med.* 22, 480–485.
- (61) Ringsdorf, H., Schlarb, B., and Venzmer, J. (1988) Molecular architecture and function of polymeric oriented systems - models for the study of organization, surface recognition, and dynamics of biomembranes. *Angew. Chem., Int. Ed.* 27, 113–158.
- (62) Kato, A., Arakawa, M., and Kondo, T. (1984) Preparation and stability of liposome-type artificial red blood cells stabilized with carboxymethylchitin. *J. Microencapsul.* 1, 105–112.
- (63) Mobed, M., Nishiya, T., and Chang, T. M. (1992) Preparation of carboxymethylchitin-incorporated submicron bilayer-lipid membrane artificial cells (liposomes) encapsulating hemoglobin. *Biomater. Artif. Cells Immobil. Biotechnol.* 20, 365–368.
- (64) Li, S., Nickels, J., and Palmer, A. F. (2005) Liposome-encapsulated actin-hemoglobin (LEAChb) artificial blood substitutes. *Biomaterials* 26, 3759–3769.
- (65) Tsuchida, E., Hasegawa, E., Kimura, N., Hatashita, M., and Makino, C. (1992) Polymerization of unsaturated phospholipids as large unilamellar liposomes at low temperature. *Macromolecules* 25, 2007–212.
- (66) Sakai, H., Takeoka, S., Yokohama, H., Nishide, H., and Tsuchida, E. (1992) Encapsulation of Hb into unsaturated lipid vesicles and gamma-ray polymerization. *Polym. Adv. Technol.* 3, 389–394.
- (67) Akama, K., Awai, K., Yano, Y., Tokuyama, S., and Nakano, Y. (2000) In vitro and in vivo stability of polymerized mixed liposomes composed of 2,4-octadecadienoyl groups of phospholipids. *Polym. Adv. Technol.* 11, 280–287.
- (68) Sakai, H., Takeoka, S., Park, S. I., Kose, T., Nishide, H., Izumi, Y., Yoshizu, A., Kobayashi, K., and Tsuchida, E. (1997) Surface-modification of hemoglobin vesicles with poly(ethylene glycol) and effects on aggregation, viscosity, and blood flow during 90%-exchange transfusion in anesthetized rats. *Bioconjugate Chem.* 8, 23–30.
- (69) Sakai, H., Tsai, A. G., Kerger, H., Park, S. I., Takeoka, S., Nishide, H., Tsuchida, E., and Intaglietta, M. (1998) Subcutaneous microvascular responses to hemodilution with red cell substitutes consisting of polyethylene glycol-modified vesicles encapsulating hemoglobin. *J. Biomed. Mater. Res.* 40, 66–78.
- (70) Sakai, H., Okamoto, M., Ikeda E., Horinouchi H., Kobayashi K., and Tsuchida, E. (2008) Histopathological changes of rat brain after direct injection of hemoglobin vesicles (oxygen carriers) and neurological impact in an intracerebral hemorrhage model. *J. Biomed. Mater. Res., Part A* (in press).
- (71) Sakai, H., Tomiyama, K., Sou, K., Takeoka, S., and Tsuchida, E. (2000) Poly(ethylene glycol)-conjugation and deoxygenation enable long-term preservation of hemoglobin vesicles as oxygen carriers in a liquid state. *Bioconjugate Chem.* 11, 425–432.
- (72) Sou, K., Endo, T., Takeoka, S., and Tsuchida, E. (2000) Poly(ethylene glycol)-modification of the phospholipid vesicles by using the spontaneous incorporation of poly(ethylene glycol)-lipid into the vesicles. *Bioconjugate Chem.* 11, 372–379.
- (73) Sato, T., Sakai, H., Sou, K., Buchner, R., and Tsuchida, E. (2007) Poly(ethylene glycol)-conjugated phospholipids in aqueous micellar solutions: hydration, static structure, and interparticle interactions. *J. Phys. Chem. B* 111, 1393–1401.
- (74) Szebeni, J. (2005) Complement activation-related pseudoallergy: a new class of drug-induced acute immune toxicity. *Toxicology* 216, 106–121.
- (75) Van de Velde, M., Wouters, P. F., Rolf, N., Van Aken, H., and Vandermeersch, E. (1998) Comparative hemodynamic effects of three different parenterally administered lipid emulsions in conscious dogs. *Crit. Care Med.* 26, 132–137.
- (76) Vercellotti, G. M., Hammerschmidt, D. E., Craddock, P. R., and Jacob, H. S. (1982) Activation of plasma complement by perfluorocarbon artificial blood: probable mechanism of adverse pulmonary reactions in treated patients and rationale for corticosteroids prophylaxis. *Blood* 59, 1299–1304.
- (77) Phillips, W. T., Klipper, R., Fresne, D., Rudolph, A. S., Javors, M., and Goins, B. (1997) Platelet reactivity with liposome-encapsulated hemoglobin in the rat. *Exp. Hematol.* 25, 1347–1356.



- (78) Szebeni, J., Fontana, J. L., Wassef, N. M., Mongan, P. D., Morse, D. S., Dobbins, D. E., Stahl, G. L., Bunger, R., and Alving, C. R. (1999) Hemodynamic changes induced by liposomes and liposome-encapsulated hemoglobin in pigs: a model for pseudoallergic cardiopulmonary reactions to liposomes. Role of complement and inhibition by soluble CR1 and anti-C5a antibody. *Circulation* 99, 2302–2309.
- (79) Izumi, Y., Sakai, H., Kose, T., Hamada, K., Takeoka, S., Yoshizu, A., Horinouchi, H., Kato, R., Nishide, H., Tsuchida, E., and Kobayashi, K. (1997) Evaluation of the capabilities of a hemoglobin vesicle as an artificial oxygen carrier in a rat exchange transfusion model. *ASAIO J.* 43, 289–297.
- (80) Loughrey, H. C., Bally, M. B., Reinish, L. W., and Cullis, P. R. (1990) The binding of phosphatidylglycerol liposomes to rat platelets is mediated by complement. *Thromb. Haemost.* 64, 172–176.
- (81) Chonn, A., Cullis, P. R., and Devine, D. V. (1991) The role of surface charge in the activation of the classical and alternative pathways of complement by liposomes. *J. Immunol.* 146, 4234–4241.
- (82) Sou, K., and Tsuchida, E. (2008) Electrostatic interactions and complement activation on the surface of phospholipid vesicle containing acidic lipids: effect of the structure of acidic groups. *Biochim. Biophys. Acta - Biomembr.* 1778, 1035–1041.
- (83) Abe, H., Azuma, H., Yamaguchi, M., Fujihara, M., Ikeda, H., Sakai, H., Takeoka, S., and Tsuchida, E. (2007) Effects of hemoglobin vesicles, a liposomal artificial oxygen carrier, on hematological responses, complement and anaphylactic reactions in rats. *Artif. Cells Blood Substit. Biotechnol.* 35, 157–172.
- (84) Abe, H., Fujihara, M., Azuma, H., Ikeda, H., Ikebuchi, K., Takeoka, S., Tsuchida, E., and Harashima, H. (2006) Interaction of hemoglobin vesicles, a cellular-type artificial oxygen carrier, with human plasma: effects on coagulation, kallikrein-kinin, and complement systems. *Artif. Cells Blood Substit. Immobil. Biotechnol.* 34, 1–10.
- (85) Wakamoto, S., Fujihara, M., Abe, H., Yamaguchi, M., Azuma, H., Ikeda, H., Takeoka, S., and Tsuchida, E. (2005) Effects of hemoglobin vesicles on resting and agonist-stimulated human platelets *in vitro*. *Artif. Cells Blood Substit. Immobil. Biotechnol.* 33, 101–111.
- (86) Wakamoto, S., Fujihara, M., Abe, H., Sakai, H., Takeoka, S., Tsuchida, E., Ikeda, H., and Ikebuchi, K. (2001) Effects of poly(ethyleneglycol)-modified hemoglobin vesicles on agonist-induced platelet aggregation and RANTES release *in vitro*. *Artif. Cells Blood Substit. Immobil. Biotechnol.* 29, 191–201.
- (87) Takeoka, S., Mori, K., Ohkawa, H., Sou, K., and Tsuchida, E. (2000) Synthesis and assembly of poly(ethylene glycol)-lipids with mono-, di-, and tetraacyl chains and a poly(ethylene glycol) chain of various molecular weights. *J. Am. Chem. Soc.* 122, 7927–7935.
- (88) Okamura, Y., Maekawa, I., Teramura, Y., Maruyama, H., Handa, M., Ikeda, Y., and Takeoka, S. (2005) Hemostatic effects of phospholipid vesicles carrying fibrinogen gamma chain dodecapeptide *in vitro* and *in vivo*. *Bioconjugate Chem.* 16, 1589–1596.
- (89) Ohkawa, H., Teramura, Y., Takeoka, S., and Tsuchida, E. (2000) Synthesis of multiacyl poly(ethylene glycol) for the conjugation of cytochrome c to phospholipid vesicle. *Bioconjugate Chem.* 11, 815–821.
- (90) Sou, K., Goins, B., Takeoka, S., Tsuchida, E., and Phillips, W. T. (2007) Selective uptake of surface-modified phospholipid vesicles by bone marrow macrophages *in vivo*. *Biomaterials* 28, 2655–2666.
- (91) Teramura, Y., and Iwata, H. (2008) Islets surface modification prevents blood-mediated inflammatory responses. *Bioconjugate Chem.* 19, 1389–1395.
- (92) Obata, Y., Suzuki, D., and Takeoka, S. (2008) Evaluation of cationic assemblies constructed with amino acid based lipids for plasmid DNA delivery. *Bioconjugate Chem.* 19, 1055–1063.
- (93) Sou, K., Inenaga, S., Takeoka, S., and Tsuchida, E. (2008) Loading of curcumin into macrophages using lipid-based nanoparticles. *Int. J. Pharm.* 352, 287–293.
- (94) Sou, K., Klipper, R., Goins, B., Tsuchida, E., and Phillips, W. T. (2005) Circulation kinetics and organ distribution of Hb vesicles developed as a red blood cell substitute. *J. Pharmacol. Exp. Ther.* 312, 702–709.
- (95) Bradley, A. J., Devine, D. V., Ansell, S. M., Janzen, J., and Brooks, D. E. (1998) Inhibition of liposome-induced complement activation by incorporated poly(ethylene glycol)-lipids. *Arch. Biochem. Biophys.* 357, 185–194.
- (96) Hu, Q., and Liu, D. (1996) Co-existence of serum-dependent and serum-independent mechanisms for liposome clearance and involvement of non-Kupffer cells in liposome uptake by mouse liver. *Biochim. Biophys. Acta* 1284, 153–161.
- (97) Shibuya-Fujiwara, N., Hirayama, F., Ogata, Y., Ikeda, H., and Ikebuchi, K. (2001) Phagocytosis *in vitro* of polyethylene glycol-modified liposome-encapsulated hemoglobin by human peripheral blood monocytes plus macrophages through scavenger receptors. *Life Sci.* 70, 291–300.
- (98) Sakai, H., Horinouchi, H., Tomiyama, K., Ikeda, E., Takeoka, S., Kobayashi, K., and Tsuchida, E. (2001) Hemoglobin-vesicles as oxygen carriers: influence on phagocytic activity and histopathological changes in reticuloendothelial system. *Am. J. Pathol.* 159, 1079–1088.
- (99) Sakai, H., Horinouchi, H., Masada, Y., Takeoka, S., Kobayashi, K., and Tsuchida, E. (2004) Metabolism of hemoglobin-vesicles (artificial oxygen carriers) and their influence on organ functions in a rat model. *Biomaterials* 25, 4317–4325.
- (100) Sakai, H., Masada, Y., Horinouchi, H., Ikeda, E., Sou, K., Takeoka, S., Suematsu, M., Takaori, M., Kobayashi, K., and Tsuchida, E. (2004) Physiologic capacity of reticuloendothelial system for degradation of hemoglobin-vesicles (artificial oxygen carriers) after massive intravenous doses by daily repeated infusions for 14 days. *J. Pharmacol. Exp. Ther.* 311, 874–884.
- (101) Sakai, H., Horinouchi, H., Yamamoto, M., Ikeda, E., Takeoka, S., Takaori, M., Tsuchida, E., and Kobayashi, K. (2006) Acute 40% exchange-transfusion with hemoglobin-vesicles (HbV) suspended in recombinant human serum albumin solution: degradation of HbV and erythropoiesis in a rat spleen for 2 weeks. *Transfusion* 46, 339–347.
- (102) Sakai, H., Seishi, Y., Obata, Y., Takeoka, S., Horinouchi, H., Tsuchida, E., and Kobayashi, K. (2009) Fluid resuscitation with artificial oxygen carriers in hemorrhaged rats: Profiles of hemoglobin-vesicle degradation and hematopoiesis for 14 days. *Shock* 31, 192–200.
- (103) Yamaoka, T., Tabata, Y., and Ikada, Y. (1994) Distribution and tissue uptake of poly(ethylene glycol) with different molecular weights after intravenous administration to mice. *J. Pharm. Sci.* 83, 601–606.
- (104) Ohki, N., Kimura, T., and Ogata, Y. (1998) The reduction of methemoglobin in Neo Red Cell. *Artif. Cells Blood Substit. Immobil. Biotechnol.* 26, 477–485.
- (105) Sakai, H., Tsai, A. G., Rohlf, R. J., Hara, H., Takeoka, S., Tsuchida, E., and Intaglietta, M. (1999) Microvascular responses to hemodilution with Hb vesicles as red cell substitutes: Influences of O<sub>2</sub> affinity. *Am. J. Physiol. Heart Circ. Physiol.* 276, H553–H562.
- (106) Wang, L., Morizawa, K., Tokuyama, S., Satoh, T., and Tsuchida, E. (1992) Modulation of oxygen-carrying capacity of artificial red cells (ARC). *Polym. Adv. Technol.* 4, 8–11.
- (107) Cabrales, P., Sakai, H., Tsai, A. G., Takeoka, S., Tsuchida, E., and Intaglietta, M. (2005) Oxygen transport by low and normal oxygen affinity hemoglobin vesicles in extreme hemodilution. *Am. J. Physiol. Heart Circ. Physiol.* 288, H1885–H1892.
- (108) Izumi, Y., Sakai, H., Hamada, K., Takeoka, S., Yamahata, T., Kato, R., Nishide, H., Tsuchida, E., and Kobayashi, K. (1996) Physiologic responses to exchange transfusion with hemoglobin vesicles as an artificial oxygen carrier in anesthetized rats: changes in mean arterial pressure and renal cortical oxygen tension. *Crit. Care Med.* 24, 1869–1873.

- (109) Sakai, H., Takeoka, S., Wettstein, R., Tsai, A. G., Intaglietta, M., and Tsuchida, E. (2002) Systemic and Microvascular responses to the hemorrhagic shock and resuscitation with Hb vesicles. *Am. J. Physiol. Heart Circ. Physiol.* 283, H1191–H1199.
- (110) Sakai, H., Masada, Y., Horinouchi, H., Yamamoto, M., Ikeda, E., Takeoka, S., Kobayashi, K., and Tsuchida, E. (2004) Hemoglobin vesicles suspended in recombinant human serum albumin for resuscitation from hemorrhagic shock in anesthetized rats. *Crit. Care Med.* 32, 539–545.
- (111) Yoshizu, A., Izumi, Y., Park, S. I., Sakai, H., Takeoka, S., Horinouchi, H., Ikeda, E., Tsuchida, E., and Kobayashi, K. (2004) Hemorrhagic shock resuscitation with an artificial oxygen carrier hemoglobin vesicle (HbV) maintains intestinal perfusion and suppresses the increase in plasma necrosis factor alpha (TNF $\alpha$ ). *ASAIO J.* 50, 458–463.
- (112) Terajima, K., Tsueshita, T., Sakamoto, A., and Ogawa, R. (2006) Fluid resuscitation with hemoglobin vesicles in a rabbit model of acute hemorrhagic shock. *Shock* 25, 184–189.
- (113) Yamazaki, M., Aeba, R., Yozu, R., and Kobayashi, K. (2006) Use of hemoglobin vesicles during cardiopulmonary bypass priming prevents neurocognitive decline in rats. *Circulation* 114 (1 Suppl), I220–I225.
- (114) Tsai, A. G., Vandegriff, K. D., Intaglietta, M., and Winslow, R. M. (2003) Targeted O<sub>2</sub> delivery by low-P<sub>50</sub> hemoglobin: a new basis for O<sub>2</sub> therapeutics. *Am. J. Physiol. Heart Circ. Physiol.* 285, H1411–H1419.
- (115) Plock, J. A., Tromp, A. E., Contaldo, C., Spanholtz, T., Sinovic, D., Sakai, H., Tsuchida, E., Leunig, M., Banic, A., and Erni, D. (2007) Hemoglobin vesicles reduce hypoxia-related inflammation in critically ischemic hamster flap tissue. *Crit. Care Med.* 35, 899–905.
- (116) Nolte, D., Pickelmann, S., Lang, M., Keipert, P., and Messmer, K. (2000) Compatibility of different colloid plasma expanders with perflubron emulsion: an intravital microscopic study in the hamster. *Anesthesiology* 93, 1261–1270.
- (117) Jouan-Hureau, V., Audonnet-Blaise, S., Lacatusu, D., Krafft, M. P., Dewachter, P., Cauchois, G., Stoltz, J. F., Longrois, D., and Menu, P. (2006) Effects of a new perfluorocarbon emulsion on human plasma and whole-blood viscosity in the presence of albumin, hydroxyethyl starch, or modified fluid gelatin: an *in vitro* rheologic approach. *Transfusion* 46, 1892–1898.
- (118) Vandegriff, K. D., McCarthy, M., Rohlf, R. J., and Winslow, R. M. (1997) Colloid osmotic properties of modified hemoglobins: chemically cross-linked versus polyethylene glycol surface-conjugated. *Biophys. Chem.* 69, 23–30.
- (119) Kobayashi, K. (2006) Summary of recombinant human serum albumin development. *Biologicals* 34, 55–59.
- (120) Meyuhas, D., Nir, S., and Lichtenberg, D. (1996) Aggregation of phospholipid vesicles by water-soluble polymers. *Biophys. J.* 71, 2602–2612.
- (121) Neu, B., and Meiselman, H. J. (2002) Depletion-mediated red blood cell aggregation in polymer solutions. *Biophys. J.* 83, 2482–2490.
- (122) Sakai, H., Sato, A., Takeoka, S., and Tsuchida, E. (2007) Rheological property of hemoglobin vesicles (artificial oxygen carriers) suspended in a series of plasma substitute aqueous solutions. *Langmuir* 23, 8121–8128.
- (123) Tsai, A. G., Friesenecker, B., McCarthy, M., Sakai, H., and Intaglietta, M. (1998) Plasma viscosity regulates capillary perfusion during extreme hemodilution in hamster skinfold model. *Am. J. Physiol. Heart Circ. Physiol.* 275, H2170–H2180.
- (124) Intaglietta, M., Cabrales, P., and Tsai, A. G. (2006) Microvascular perspective of oxygen-carrying and -noncarrying blood substitutes. *Annu. Rev. Biomed. Eng.* 8, 289–321.
- (125) Rebel, A., Ulatowski, J. A., Kwansa, H., Bucci, E., and Koehler, R. C. (2003) Cerebrovascular response to decreased hematocrit: effect of cell-free hemoglobin, plasma viscosity, and CO<sub>2</sub>. *Am. J. Physiol. Heart Circ. Physiol.* 285, H1600–H1608.
- (126) Dimino, M. L., and Palmer, A. F. (2007) High O<sub>2</sub> affinity hemoglobin-based oxygen carriers synthesized via polymerization of hemoglobin with ring-opened 2-chloroethyl- $\beta$ -D-fructopyranoside and 1-o-octyl- $\beta$ -D-glucopyranoside. *Biotechnol. Bioeng.* 97, 462–472.
- (127) Plock, J. A., Contaldo, C., Sakai, H., Tsuchida, E., Leunig, M., Banic, A., Menger, M. D., and Erni, D. (2005) Is the Hb in Hb vesicles infused for isovolemic hemodilution necessary to improve oxygenation in critically ischemic hamster skin? *Am. J. Physiol. Heart Circ. Physiol.* 289, H2624–H2631.
- (128) Contaldo, C., Plock, J., Sakai, H., Takeoka, S., Tsuchida, E., Leunig, M., Banic, A., and Erni, D. (2005) New generation of hemoglobin-based oxygen carriers evaluated for oxygenation of critically ischemic hamster flap tissue. *Crit. Care Med.* 33, 806–812.
- (129) Verdu, E. F., Bercik, P., Huang, X. X., Lu, J., Al-Mutawaly, N., Sakai, H., Tompkins, T. A., Croitoru, K., Tsuchida, E., Perdue, M., and Collins, S. M. (2008) The role of luminal factors in the recovery of gastric function and behavioral changes after chronic *Helicobacter pylori* infection. *Am. J. Physiol. Gastrointest. Liver Physiol.* 295, G664–G670.
- (130) Komatsu, H., Furuya, T., Sato, N., Ohta, K., Matsuura, A., Ohmura, T., Takagi, S., Matsuura, M., Yamashita, M., Itoda, M., Itoh, J., Horinouchi, H., and Kobayashi, K. (2007) Effect of hemoglobin vesicle, a cellular-type artificial oxygen carrier, on middle cerebral artery occlusion- and arachidonic acid-induced stroke models in rats. *Neurosci. Lett.* 421, 121–125.
- (131) Yamamoto, M., Izumi, Y., Horinouchi, H., Teramura, Y., Sakai, H., Kohno, M., Watanabe, M., Kawamura, M., Adachi, T., Ikeda, E., Takeoka, S., Tsuchida, E., Kobayashi, K. (2009) Systemic administration of hemoglobin vesicle elevates tumor tissue oxygen tension and modifies tumor response to irradiation. *J. Surg. Res.* doi:10.1016/j.jss.2007.12.770.
- (132) Sakai, H., Horinouchi, H., Tsuchida, E., Kobayashi, K. (2008) Hemoglobin-vesicles and red blood cells as carriers of carbon monoxide prior to oxygen for resuscitation after hemorrhagic shock in a rat model. *Shock*. doi:10.1097/SHK.0b013e318189017a.
- (133) Peters, T. (1996) *All about Albumin: Biochemistry, Genetics and Medical Applications*, Academic Press, San Diego.
- (134) He, X. M., and Carter, D. C. (1992) Atomic structure and chemistry of human serum albumin. *Nature* 358, 209–215.
- (135) Carter, D. C., and Ho, J. X. (1994) Structure of serum albumin. *Adv. Protein Chem.* 45, 153–203.
- (136) Curry, S., Madelkow, H., Brick, P., and Franks, N. P. (1998) Crystal structure of human serum albumin complexed with fatty acid reveals an asymmetric distribution of binding sites. *Nat. Struct. Biol.* 5, 827–835.
- (137) Bhattacharya, A. A., Grune, T., and Curry, S. (2000) Crystal structures of human serum albumin complexed with monounsaturated and polyunsaturated fatty acids. *J. Mol. Biol.* 303, 721–732.
- (138) Ghuman, J., Zunszain, P. A., Petitpas, I., Bhattacharya, A. A., Otagiri, M., and Curry, S. (2007) Structural basis of the drug-binding specificity of human serum albumin. *J. Mol. Biol.* 353, 38–52.
- (139) Tsuchida, E., Komatsu, T., Matsukawa, Y., Hamamatsu, K., and Wu, J. (1999) Human serum albumin incorporating tetrakis(o-pivalamido)phenyl porphyrinatoiron(II) derivative as a totally synthetic O<sub>2</sub>-carrying hemoprotein. *Bioconjugate Chem.* 10, 797–802.
- (140) Komatsu, T., Hamamatsu, K., Wu, J., and Tsuchida, E. (1999) Physicochemical properties and O<sub>2</sub>-coordination structure of human serum albumin incorporating tetrakis(o-pivalamido)phenylporphyrinatoiron(II) derivatives. *Bioconjugate Chem.* 10, 82–86.
- (141) Tsuchida, E., Komatsu, T., Yanagimoto, T., and Sakai, H. (2003) Preservation stability and *in vivo* administration of albumin-heme hybrid solution as an entirely synthetic O<sub>2</sub>-carrier. *Polym. Adv. Technol.* 13, 848–850.
- (142) Huang, Y., Komatsu, T., Nakagawa, A., Tsuchida, E., and Kobayashi, S. (2003) Compatibility *in vitro* of albumin-heme

- (O<sub>2</sub> carrier) with blood cell components. *J. Biomed. Mater. Res.* 66A, 292–297.
- (143) Komatsu, T., Huang, Y., Wakamoto, S., Abe, H., Fujihara, M., Azuma, H., Ikeda, H., Yamamoto, H., Horinouchi, H., and Kobayashi, K. (2007) Influence of O<sub>2</sub>-carrying plasma hemoprotein "albumin-heme" on complement system and platelet activation *in vitro* and physiological responses to exchange transfusion. *J. Biomed. Mater. Res.* 81A, 821–826.
- (144) Tsuchida, E., Nakagawa, A., and Komatsu, T. (2003) Coordination structure of active site in synthetic hemoprotein (albumin-heme) with dioxygen and carbon monoxide. *Macromol. Symp.* 195, 275–280.
- (145) Komatsu, T., Matsukawa, Y., and Tsuchida, E. (2000) Nitrosyl iron(II) complex of *meso*-tetrakis( $\alpha,\alpha,\alpha,\alpha$ -*o*-pivalamidophenyl)porphyrin with a covalently linked 2-methylimidazolylalkyl group. *Chem. Lett.* 1060–1061.
- (146) Komatsu, T., Matsukawa, Y., and Tsuchida, E. (2001) Reaction of nitric oxide with synthetic hemoprotein, human serum albumin incorporating tetraphenylporphyrinatoiron(II) derivatives. *Bioconjugate Chem.* 12, 71–75.
- (147) Collman, J. P., Brauman, J. I., Iverson, B. L., Sessler, J. L., Morris, R. M., and Gibson, Q. H. (1983) O<sub>2</sub> and CO binding to iron(II) porphyrins: A comparison of the "picket fence" and "pocket" porphyrins. *J. Am. Chem. Soc.* 105, 3052–3064.
- (148) Traylor, T. G., Tsuchiya, S., Campbell, D., Mitchell, M., Stynes, D., and Koga, N. (1985) Anthracene-heme cyclophanes. Steric in CO, O<sub>2</sub> and RNC binding. *J. Am. Chem. Soc.* 107, 604–614.
- (149) Komatsu, T., Matsukawa, Y., and Tsuchida, E. (2000) Kinetics of CO and O<sub>2</sub> binding to human serum albumin-heme hybrid. *Bioconjugate Chem.* 11, 772–776.
- (150) Komatsu, T., Matsukawa, Y., and Tsuchida, E. (2002) Effect of heme structure on O<sub>2</sub>-binding properties of human serum albumin-heme hybrids: intramolecular histidine coordination provides a stable O<sub>2</sub>-adduct complex. *Bioconjugate Chem.* 13, 397–402.
- (151) Nakagawa, A., Komatsu, T., Iizuka, M., and Tsuchida, E. (2008) O<sub>2</sub> binding to human serum albumin incorporating iron porphyrin with a covalently linked methyl-L-histidine isomer. *Bioconjugate Chem.* 19, 581–584.
- (152) Nakagawa, A., Komatsu, T., and Tsuchida, E. (2007) *meso*-Tetrakis( $\alpha,\alpha,\alpha,\alpha$ -*o*-amidophenyl) porphyrinatoiron(II) bearing a proximal histidyl group at the  $\beta$ -pyrrolic position via an acyl bond: synthesis and O<sub>2</sub> coordination in aqueous media. *Chem. Lett.* 36, 640–641.
- (153) Komatsu, T., Okada, T., Moritake, M., and Tsuchida, E. (2001) O<sub>2</sub>-binding properties of double-sided porphyrinatoiron(II)s with polar substituents and their human serum albumin hybrids. *Bull. Chem. Soc. Jpn.* 74, 1695–1702.
- (154) Nakagawa, A., Komatsu, T., Iizuka, M., and Tsuchida, E. (2006) Human serum albumin hybrid incorporating tailed porphyrinatoiron(II) in the  $\alpha,\alpha,\beta$ -conformer as an O<sub>2</sub>-binding site. *Bioconjugate Chem.* 17, 146–151.
- (155) Nakagawa, A., Komatsu, T., Ohmichi, N., and Tsuchida, E. (2003) Synthetic dioxygen-carrying hemoprotein. human serum albumin including iron(II) complex of protoporphyrin IX with an axially coordinated histidylglycyl-propionate. *Chem. Lett.* 32, 504–505.
- (156) Nakagawa, A., Komatsu, T., Ohmichi, N., and Tsuchida, E. (2004) Synthesis of protoheme IX derivatives with a covalently linked proximal base and their human serum albumin hybrids as artificial hemoprotein. *Org. Biomol. Chem.* 2, 3108–3112.
- (157) Wang, R.-M., Komatsu, T., Nakagawa, A., and Tsuchida, E. (2005) Human serum albumin bearing covalently attached iron(II) porphyrins as O<sub>2</sub>-coordination sites. *Bioconjugate Chem.* 16, 23–26.
- (158) Harris, J. M. (1992) *Poly(ethylene glycol) Chemistry: Biotechnical and Biomedical Applications* (Harris, J. M., Ed.) Plenum Press, New York.
- (159) Veronese, F. M., and Harris, J. M. (2002) Introduction and overview of peptide and protein PEGylation. *Adv. Drug Delivery Rev.* 54, 453–456.
- (160) Roberts, M. J., Bentley, M. D., and Harris, J. M. (2002) Chemistry for peptide and protein PEGylation. *Adv. Drug Delivery Rev.* 54, 459–476.
- (161) Veronese, F. M. (2001) Peptide and protein PEGylation: a review of problems and solutions. *Biomaterials* 22, 405–417.
- (162) Nucci, M. L., Shorr, R., and Abuchowski, A. (1991) The therapeutic value of poly(ethylene glycol) modified proteins. *Adv. Drug Delivery Rev.* 6, 133–151.
- (163) Kawahara, N. Y., and Ohno, H. (1997) Induced thermostability of poly(ethylene oxide)-modified hemoglobin in glycols. *Bioconjugate Chem.* 8, 643–648.
- (164) Huang, Y., Komatsu, T., Wang, R.-M., Nakagawa, A., and Tsuchida, E. (2006) Poly(ethylene glycol)-conjugated human serum albumin including iron porphyrins: surface modification improves the O<sub>2</sub>-transporting ability. *Bioconjugate Chem.* 17, 393–398.
- (165) Cabrales P., Tsai, A. G., Intaglietta, M. (2004) Microvascular pressure and functional capillary density in extreme hemodilution with low- and high-viscosity dextran and a low-viscosity Hb-based O<sub>2</sub> carrier. *Am. J. Physiol. Heart Circ. Physiol.* 287, H363–H373.
- (166) Martini, J., Cabrales, P., K, A., Acharya, S. A., Intaglietta, M., Tsai, A. G. (2008) Survival time in severe hemorrhagic shock after perioperative hemodilution is longer with PEG-conjugated human serum albumin than HES 130/0.4: a microvascular perspective. *Crit. Care* 12, R54.
- (167) Sugawara, Y., and Shikama, K. (1980) Autoxidation of native oxymyoglobin. *Eur. J. Biochem.* 110, 241–246.
- (168) Tsuchida, E., Komatsu, T., Hamamatsu, K., Matsukawa, Y., Tajima, A., Yoshizu, A., Izumi, Y., and Kobayashi, K. (2000) Exchange transfusion with albumin-heme as an artificial O<sub>2</sub>-infusion into anesthetized rats: physiological responses, O<sub>2</sub>-delivery, and reduction of the oxidized heme sites by red blood cells. *Bioconjugate Chem.* 11, 46–50.
- (169) Huang, Y., Komatsu, T., Yamamoto, H., Horinouchi, H., Kobayashi, K., and Tsuchida, E. (2006) PEGylated albumin-heme as an oxygen-carrying plasma expander: exchange transfusion into acute anemia rat model. *Biomaterials* 27, 4477–4483.
- (170) Tsuchida, E., Komatsu, T., Matsukawa, Y., Nakagawa, A., Sakai, H., Kobayashi, K., and Suematsu, M. (2003) Human serum albumin incorporating synthetic heme: red blood cell substitute without hypertension by nitric oxide scavenging. *J. Biomed. Mater. Res.* 64A, 257–261.
- (171) Nakagawa, A., Komatsu, T., Huang, H., Lu, G., and Tsuchida, E. (2007) O<sub>2</sub>-binding albumin thin films: solid membranes of poly(ethylene glycol)-conjugated human serum albumin incorporating iron porphyrin. *Bioconjugate Chem.* 18, 1673–1677.
- (172) Goa, K. L., and Benfield, P. (1994) Hyaluronic-acid - a review of its pharmacology and use as a surgical and in ophthalmology, and its therapeutic potential in joint disease and wound-healing. *Drugs* 47, 536–566.
- (173) Adams, P. A., and Berman, M. C. (1980) Kinetics and mechanism of the interaction between human serum albumin and monomeric haemin. *Biochem. J.* 191, 95–102.
- (174) Zunszain, P. A., Ghuman, J., Komatsu, T., Tsuchida, E., and Curry, S. (2003) Crystal structural analysis of human serum albumin complexed with heme and fatty acid. *BMC Struct. Biol.* 3, 6.
- (175) Wardell, M., Wang, Z., Ho, J. X., Robert, J., Ruker, F., Ruble, J., and Carter, D. C. (2002) The atomic structure of human methemalbumin at 1.9 Å. *Biochem. Biophys. Res. Commun.* 291, 813–819.
- (176) Komatsu, T., Ohmichi, N., Zunszain, P. A., Curry, S., and Tsuchida, E. (2004) Dioxygenation of human serum albumin having a prosthetic-heme group in a tailor-made heme pocket. *J. Am. Chem. Soc.* 126, 14304–14305.
- (177) Komatsu, T., Ohmichi, N., Nakagawa, A., Zunszain, P. A., Curry, S., and Tsuchida, E. (2005) O<sub>2</sub> and CO binding properties of artificial hemoproteins formed by complexing iron protoporphyrin IX with human serum albumin mutants. *J. Am. Chem. Soc.* 127, 15933–15942.
- (178) Vickery, L., Nozawa, T., and Sauer, K. (1976) Magnetic circular dichroism studies of myoglobin complexes. Correlation

- with-heme spin state and axial ligation. *J. Am. Chem. Soc.* 98, 343–350.
- (179) Antonini, E., and Brunori, M. *Hemoglobin and Myoglobin in Their Reactions with Ligands*, p 18, North-Holland Publishers, Amsterdam.
- (180) Rohlfis, R., Mathews, A. J., Carver, T. E., Olson, J. S., Springer, B. A., Egeberg, K. D., and Sligar, S. G. (1990) The effects of amino acid substitution at position E7 (residue 64) on the kinetics of ligand binding to sperm whale myoglobin. *J. Biol. Chem.* 265, 3168–3176.
- (181) Imai, K., Morimoto, H., Kotani, M., Watari, H., Hirata, W., and Kuroda, M. (1970) Studies of the function of abnormal hemoglobins I. An improved method for automatic measurement of the oxygen equilibrium curve of hemoglobin. *Biochim. Biophys. Acta* 200, 189–197.
- (182) Vandegriff, K. D., Young, M. A., Lohman, J., Bellelli, A., Samaja, M., Malavalli, A., and Winslow, R. M. (2008) CO-MP4, a polyethylene glycol-conjugated haemoglobin derivative and carbon monoxide carrier that reduces myocardial infarct size in rats. *Br. J. Pharmacol.* 154, 1649–1561.
- (183) Creighton, T. E. (1992) *Proteins: Structures and Molecular Properties*, p 242, W. H. Freeman and Co., New York.
- (184) Chu, M. M. L., Castro, C. E., and Hathaway, G. M. (1978) Oxidation of low-spin iron(II) porphyrins by molecular oxygen. An outer sphere mechanism. *Biochemistry* 17, 481–486.
- (185) Tsuchida, E., Nishide, H., Sato, Y., and Kaneda, M. (1982) The preparation of protoheme mono-N-[5-(2-methyl-1-imidazolyl)pentyl]amide and its oxygenation. *Bull. Chem. Soc. Jpn.* 55, 1890–1895.
- (186) Uno, T., Sakamoto, R., and Tomisugi, Y. (2003) Inversion of axial coordination in myoglobin to create a “proximal” ligand binding pocket. *Biochemistry* 42, 10191–10199.
- (187) Springer, B. A., Sligar, S. G., Olson, J. S., and Philips, G. N. (1994) Mechanisms of a ligand recognition in myoglobin. *Chem. Rev.* 94, 699–714.
- (188) Komatsu, T., Nakagawa, A., Zunszain, P. A., Curry, S., and Tsuchida, E. (2007) Genetic engineering of the heme pocket in human serum albumin: modulation of O<sub>2</sub> binding of iron protoporphyrin IX by variation of distal amino acids. *J. Am. Chem. Soc.* 129, 11286–11295.

BC800431D